Geological Society of America
3300 Penrose Place
P.O. Box 9140
Boulder, CO 80301
(303) 447-2020 • fax 303-357-1073
www.geosociety.org

This PDF file is subject to the following conditions and restrictions:

Copyright © 2006, The Geological Society of America, Inc. (GSA). All rights reserved. Copyright not claimed on content prepared wholly by U.S. government employees within scope of their employment. Individual scientists are hereby granted permission, without fees or further requests to GSA, to use a single figure, a single table, and/or a brief paragraph of text in other subsequent works and to make unlimited copies for noncommercial use in classrooms to further education and science. For any other use, contact Copyright Permissions, GSA, P.O. Box 9140, Boulder, CO 80301-9140, USA, fax 303-357-1073, editing@geosociety.org. GSA provides this and other forums for the presentation of diverse opinions and positions by scientists worldwide, regardless of their race, citizenship, gender, religion, or political viewpoint. Opinions presented in this publication do not reflect official positions of the Society.

Geological Society of America
Special Paper 398
2006

Escarpment erosion and landscape evolution in southeastern Australia

Arjun M. Heimsath[†]
Department of Earth Sciences, Dartmouth College, Hanover, New Hampshire 03755, USA
John Chappell
Research School of Earth Sciences, Australian National University, Canberra, ACT 0200, Australia
Robert C. Finkel
Center for Accelerator Mass Spectrometry, Lawrence Livermore National Laboratory, Livermore, California 94550, USA
Keith Fifield
Research School of Physical Sciences and Engineering, Australian National University, Canberra, ACT 0200, Australia
Abaz Alimanovic
Research School of Earth Sciences, Australian National University, Canberra, ACT 0200, Australia

ABSTRACT

Passive margin escarpments are extensively studied around the world, and understanding their evolution continues to present one of the more compelling interdisciplinary challenges tackled by earth scientists today. Escarpments reflect the morphotectonic development of passive margins and can separate regions with different climatic histories, but the inferred rapid rates of escarpment retreat have been at odds with actual measurements of land surface denudation. In this paper we present results from extensive cosmogenic ^{10}Be and ^{26}Al analyses across the escarpment of southeastern Australia to quantify the erosional processes evolving the highland, lowland, and scarp face landscapes. We document new relationships between soil production rates and soil thicknesses for the highland and lowland landscapes and compare these soil production functions with those published in our earlier studies from the highlands and at the base of the escarpment. Both new functions define exponential declines of soil production rates with increasing soil depths, with inferred intercepts of 65 and 42 m/m.y. for the highland and lowland sites, respectively, and slopes of –0.02. Exposed bedrock at both of the new sites erodes more slowly than the maximum soil production rates, at 22 ± 3 and 9 ± 2 m/m.y., respectively, thus suggesting a "humped" soil production function. We suggest that instead of a humped function, lithologic variations set the emergence of bedrock, which evolves into the tors that are found extensively across the highlands and at the crest of the escarpment by eroding more slowly than the surrounding soil-mantled landscape. Compared to soil production rates from previous work using ^{10}Be and ^{26}Al measurements from two different sites, these results show remarkable agreement and specifically quantify a soil production function for the region where soil production rates decline exponentially with increasing soil thickness, with an intercept of 53 m/m.y. and a slope of –0.02. Erosion rates determined from ^{10}Be concentrations from outcropping tors, bedrock, and saprolite from a main spur ridge perpendicular to the escarpment, and sediments from first- and zero-order catchments draining the main ridges, show a clear

[†]E-mail: arjun.heimsath@dartmouth.edu.

Heimsath, A.M., Chappell, J., Finkel, R.C., Fifield, K., and Alimanovic, A., 2006, Escarpment erosion and landscape evolution in southeastern Australia, *in* Willett, S.D., Hovius, N., Brandon, M.T., and Fisher, D.M., eds., Tectonics, Climate, and Landscape Evolution: Geological Society of America Special Paper 398, Penrose Conference Series, p. 173–190, doi: 10.1130/2006.2398(10). For permission to copy, contact editing@geosociety.org. ©2006 Geological Society of America.

linear decline with elevation, from ~35 m/m.y. near the escarpment base to ~3 m/m.y. at the escarpment crest. This order of magnitude difference in erosion rates may be due to increases in stream incision with distance downslope on the escarpment, or to decreases in precipitation with elevation, neither of which we quantify here. The rates do agree, in general, with our soil production functions, suggesting that the biogenic processes actively eroding soil-mantled landscapes are shaping the evolution of the escarpment despite our observations of block fall and debris-flow processes across the steep regions near the scarp crest. Our results support recent results from studies using low-temperature thermochronology, which suggest that the escarpment is relatively stable after having retreated rapidly immediately following rifting. Differences between our rates of surface erosion caused by processes active today and the scarp retreat rates needed to place the escarpment in its present position need to be explained by future work to untangle the mysteries of escarpment evolution.

Keywords: cosmogenic nuclides, altitudinal transect, tectonic geomorphology, scarp evolution.

INTRODUCTION

Passive continental margins and the escarpments that are typically associated with them have captured the attention of much geomorphic study, helping to build the application of numerical modeling as well as develop applications of new analytical techniques in the field of quantitative geomorphology (e.g., Bierman and Caffee, 2001; Cockburn et al., 2000; King, 1962; Ollier, 1982; Summerfield, 1999; Tucker and Slingerland, 1994; van der Beek and Braun, 1998). Interest in escarpments is well founded, as understanding landscape evolution of a passive margin escarpment forces an integration of climate, tectonic, and surface process studies. Traditional views of escarpment evolution have suggested high rates of escarpment retreat, parallel to the continental margin, in comparison with low rates of denudation in the low-relief highlands as well as across the more highly dissected lowlands.

Despite such long-standing interest in understanding the evolution of passive margin escarpments, relatively few data actually quantify the rates of surface erosion and long-term denudation across these margins to confirm qualitative models of rapid escarpment retreat. Recent work using low-temperature thermochronology place critical long-term constraints on escarpment denudation (e.g., Brown et al., 2002; Cockburn et al., 2000; Persano et al., 2002), while cosmogenic nuclides have defined shorter-term surface erosion rates above (Heimsath et al., 2001), across (Bierman and Caffee, 2001; Cockburn et al., 2000), and below (Heimsath et al., 2000) escarpments in southeastern Australia and Namibia. These data refute the traditional models of escarpment evolution, and instead suggest that relatively rapid rates of postrifting denudation are followed by long periods of lower erosion rates and the development of a long-term steady-state in the topographic form of the escarpment, where relatively slow landscape change is occurring.

We tackle the problem of escarpment evolution by applying the well-developed mass-balance approach initially articulated by Gilbert (1877), quantitatively laid out by Culling (1960, 1965), and eloquently made accessible to a broad audience by Carson and Kirkby (1972). This conceptual framework has been extensively applied recently to quantify soil production (e.g., Heimsath et al., 1997, 1999), landscape evolution (e.g., Dietrich et al., 1995), as well as model the dynamic responses of the land surface to changes in climate and tectonic forcing (e.g., Tucker and Slingerland, 1997; van der Beek and Braun, 1999). Specifically, we are interested in the vertical lowering rate of the land surface. For a bedrock surface, this rate is simply the erosion rate of the surface. For a soil-mantled landscape, this is the rate of conversion of the underlying weathered bedrock to mobile material: the soil production rate. Soil production rates have been hypothesized and recently documented to decline exponentially with increasing soil thickness in a relationship termed the soil production function (Heimsath et al., 1997). Note that soil production rates only equal total erosion rates (including solute loss), i.e., landscape lowering rates relative to a local datum, if local soil thickness is roughly constant over time. This conceptual framework applies to upland, soil-mantled landscapes with no recent history of glaciation, without significant eolian deposition, and only across divergent (convex-up) noses where there is no net soil deposition (Dietrich et al., 1995; Heimsath et al., 1997, 1999). Field verification of this function helps quantify recent landscape evolution models (Dietrich et al., 2003), and the local steady-state soil thickness assumption was verified at one of the field areas used here (Heimsath et al., 2000).

In this paper we present new results from a comprehensive study done across the passive margin escarpment (cf. Great Escarpment; Ollier, 1982) of southeastern Australia. We use two in situ–produced cosmogenic nuclides, ^{10}Be and ^{26}Al, to quantify erosion rates and processes from the low-relief coastal lowlands to the highlands above the escarpment. These erosion rates are compared with two new, well-defined, soil production functions that we present from the highlands at the escarpment crest and from the coastal lowlands. These soil production functions illustrate differences in the processes eroding the highlands in comparison with the coastal lowlands and escarpment base. These 44

new cosmogenic nuclide data are used with two independent data sets published using cosmogenic nuclides and landscape morphology from the base of the escarpment and from the highlands above the escarpment to show that erosion rates decrease with elevation from escarpment base to crest and that soil production rates decrease exponentially with increasing soil thickness. Our findings are consistent with recent studies (e.g., Cockburn et al., 2000; Matmon et al., 2002; Persano et al., 2002; van der Beek et al., 2002) that concluded that passive margin escarpments have been relatively stable and are not retreating as rapidly as suggested by earlier studies of escarpment evolution. To place our results in the context of the extensive work done to understand landscape evolution across the southeastern Australia rift margin, we begin with a brief review.

ERODING AND EVOLVING THE ESCARPMENT

The passive continental margin of southeastern Australia provides an excellent example of a landscape where the processes and rates of evolution have been studied over multiple time scales (e.g., Bishop, 1988; Dumitru et al., 1995; Lambeck and Stephenson, 1985; Nott, 1992; O'Sullivan et al., 1996; Ollier, 1995; Persano et al., 2002; Seidl et al., 1996; Stephenson and Lambeck, 1985; van der Beek and Braun, 1998; Wellman, 1987). This margin is thought to have begun with the rifting between the Australian continent and the Lord Howe Rise to the east ca. 85–100 Ma (Hayes and Ringis, 1973; Weissel and Hayes, 1977). While there has been much debate about the subsequent uplift, erosion, and evolution of the landscape associated with this rift, the large-scale morphology is roughly similar to other passive margins around the world (Matmon et al., 2002), although an important difference exists in that the drainage divide occurs inland of the scarp crest. The highland region of gentle topography, low-relief, and relatively slow erosion rates (e.g., Bishop, 1986; Bishop and Brown, 1992; Bishop et al., 1985; Nott, 1992; Ollier, 1978; Pain, 1985; Wellman, 1987) is separated from the more deeply incised coastal belt by what was once commonly referred to as the Great Escarpment (Ollier, 1982). Modeling of the evolution of the escarpment is extensive (e.g., Lambeck and Stephenson, 1985; van der Beek and Braun, 1998) and depends on field determination of erosion rates, but much modeling of this and other escarpments has been done without empirical constraints on relevant time scales.

Slow rates of Tertiary erosion were deduced for the southeastern highlands, west of the escarpment, in several studies by dividing the age of plateau-forming basalt flows into the elevation difference between the plateau and the channels that had incised through the flows (Bishop, 1985; Bishop et al., 1985; Wellman, 1979, 1987; Wellman and McDougall, 1974). Because of the likely posteruption erosion of the basalt surface, the rates calculated were the minimum rates of incision. All of the studies deduced rates less than 10 m/m.y., with significant uncertainty, for the southeastern highlands, and slight differences depended on the time since basalt emplacement. Young (1983) and Young and McDougall (1982, 1993) extended the examination of river incision through dated basalts to infer slow rates of scarp retreat both west and east of the Great Escarpment, suggesting rates as low as 18 m/m.y.

The approach of determining long-term denudation rates for the region by using low-temperature thermochronology measured across the southeastern highlands, as well as along the present coastline, was pursued relatively early, though often with few data (Dumitru et al., 1991, 1995; Foster and Gleadow, 1991; O'Sullivan et al., 1995, 1996). These studies were motivated, at least in part, by debate over the origin, not the erosion rates, of the southeastern highlands. O'Sullivan et al. (1995, 1996) used apatite fission-track thermochronology (AFTT) to deduce two separate periods of rapid denudation based on distinct periods of rapid cooling recorded in the apatite. They suggested that the initial continental extension associated with the splitting of the Tasman Sea in the mid-Cretaceous resulted in kilometer-scale (>2 km) denudation across much of the present-day southeastern highlands, possibly due to rock uplift following underplating inland from the rift. The second period of cooling recorded in samples from the coastal regions was several tens of millions of years later, associated with the continental breakup during the Late Cretaceous (ca. 80 Ma) through the Paleocene (ca. 60 Ma). These results implied that the highlands that were uplifted and highly eroded 90–100 Ma and the more recently eroded coastal belt arrived at a position near their present morphologies ca. 60 Ma. As Bishop (1986) pointed out, most of the models of the history of the southeast Australian highlands (as opposed to models of the evolution of the continental margin) implied a stable continental divide, which roughly coincided with the Great Escarpment. The inferred tectonic processes leading to the stability of this divide and the southeastern highlands were not stated, but the conclusions regarding very slow Tertiary denudation rates on the highlands were similar to those drawn from a passive isostatic rebound model as presented by Stephenson and Lambeck (1985). Closer examination of O'Sullivan et al.'s research (1995, 1996) shows few data from potentially anomalous areas, and the supposed peak in denudation rates on the coastal strip is not supported by numerous data from other regions (Gleadow et al., 2002; van der Beek et al., 2001). Recent AFTT work (Persano et al., 2002) concludes that the highlands have been tectonically stable with relatively constant denudation rates throughout continental breakup, and suggests erosion rates <10 m/m.y. since the late Paleozoic–early Mesozoic, similar to findings by Bishop and Goldrick (2000) and Moore et al. (1986).

Slow denudation rates are part of the assumed conditions used by Thomas (1989a, 1989b, 1995), Twidale (1971, 1985, 1993), and Twidale and Vidal Romani (1994) to suggest the differential weathering processes leading to the formation of relief in some landscapes, as well as features such as inselbergs and tors. The etching process reported by these authors involves the development of a saprolite (chemically weathered rock that retains its relict structure but has not been physically transported) resulting from the prolonged interaction of groundwater with the underly-

ing bedrock. The weathering front progresses into the bedrock, penetrating into fractures and joints, and weathers the bedrock preferentially into saprolite and core-stones. Saprolite may then be stripped (for reasons and by processes not specified by these authors, but potential mechanisms could include climate change to a wetter, more humid period likely to cause higher rates of erosion) to expose the differentially weathered bedrock, resulting in the formation of relief in the landscape. Depending on the spacing of the bedrock fractures and joints, the exposure of the core-stones may result in the formation of landscape features as diverse as tors, inselbergs, angular turrets, or granite domes.

Seidl et al. (1996) and Weissel and Seidl (1997) focused on the mechanisms for propagation of the escarpment inland following the splitting of the Tasman Sea. They used a mass-balance approach to estimate denudation rates ranging from 0.04 m/m.y. to 12 m/m.y. east (downstream, or below) of the escarpment since the time of rifting. These rates were consistent with the minimum estimates of Dumitru et al. (1991), despite the rough constraints on their measurements and their assumption of initial topography, which was not substantiated. They also inferred escarpment retreat rates (Seidl et al., 1996) by dividing the average distance of many gorge heads from the rift margin (200 km) by the period since rifting (100 m.y.) to get a long-term average rate of 2 km/m.y. This rate agreed roughly with retreat rates cited from other passive continental margins (Ollier and Marker, 1985), though the same simple assumptions were used, and the reasoning was not mechanistic.

Weissel and Seidl's (1998) analyses of cosmogenic nuclide measurements from bedrock rivers determined bedrock incision rates of ~7 m/m.y. from upstream of the edge of the escarpment (which agrees with highland denudation rates of 1–10 m/m.y. for the highlands), and greater than 100 m/m.y. inferred from strath terraces downstream of the escarpment knickpoint. As they point out, their rates were consistent with their models of escarpment propagation across the coastal region with very low rates of erosion from the highland region (~4 m/m.y.), higher rates of bedrock channel incision near the upper edge of the escarpment than from upstream (~20 m/m.y. versus ~7 m/m.y.), and the highest erosion rates across the gorge head (~100 m/m.y.). Importantly, both studies (Seidl et al., 1996, and Weissel and Seidl, 1998) forward a process-based argument for the propagation of the escarpment. They suggested that as long as there is enough fluvial transport power in the streams, the propagation rate of the escarpment is primarily determined by the slope failure mechanisms and the mass wasting from the steep rock slopes at the escarpment head (also note modeling results of Tucker and Slingerland [1994], which suggested that weathering-limited conditions across the escarpment knickpoint set the retreat rate of the escarpment).

In contrast with the extensive research on the evolution and denudation of the southeastern highlands, there is a paucity of data addressing the erosional history of the coastal plain, and work that has been done appears fraught with equivocation. The notable exceptions were the low-temperature thermochronology studies that found a discrete period of rock cooling from rock samples along the coast (O'Sullivan et al., 1995, 1996; Persano et al., 2002). Perhaps one reason there have been few studies similar to those carried out on the highlands is that the retreat of the escarpment has eroded most of the material used in the earlier studies, so they must now use datable basalts to infer the evolution of the highlands from the coastal region. While the highly dissected region adjacent to and below the escarpment suggests high erosion rates, the actual rates have not been well quantified beyond a few recent studies (Heimsath et al., 2000; Persano et al., 2002; Weissel and Seidl, 1998).

Young (1977) did, however, report mantles of Tertiary sediment, duricrust, and basalt on the coastal lowlands at the foot of the escarpment. Young and McDougall (1982) reported further on this work and used datable rock to report K-Ar ages averaging ca. 30 Ma from basalt flows that postdate the silcrete formation on the lowland sites. They used the basalt ages in relation with the silcrete development to conclude that the coastal lowland resulted from erosion following an early Tertiary uplift of the highland. Similarly, based on terrestrial sedimentary deposits examined along the southeastern coast, Nott et al. (1991) concluded that the uplift of the highland region and the development of the coastal lowland occurred by the early Tertiary. They proposed that a late Mesozoic period of deep weathering was followed by an early Tertiary period of uplift and erosion. Subsequently, by the early Miocene (ca. 22 Ma), global sea-level rise may have led to a period of deposition of sediments on the present coastal plain. These aggraded sediments were exposed when the drop in sea level in the late Miocene to Pliocene (ca. 8 Ma) allowed the incision of streams into the coastal landscape. There is considerable dispute surrounding these lowland studies.

FIELD SITES

To quantify erosion rates and processes across the escarpment, we extended the field area that was used to quantify soil production rates with in situ–produced cosmogenic nuclides (^{10}Be and ^{26}Al; Heimsath et al., 2000; Figs. 1 and 2). Results from the Heimsath et al.'s (2000) study were later compared to soil production and erosion rates determined at a site on the highlands (Heimsath et al., 2001), but the highland site was roughly 60 km northwest of the escarpment base site and ~12 km west of the escarpment crest. For the study presented here, we directly connect the coastal lowland with the escarpment by sampling along ridge and river transects (Fig. 3), as well as extensive new sampling on the highlands at the escarpment lip and also on the coastal lowlands. Sampling at the escarpment lip and on the highlands near Brown Mountain was also motivated by the desire to couple our quantification of physical erosion rates with recent and ongoing work into chemical weathering in the same field region (Banfield and Eggleton, 1989; Taunton et al., 2000a, 2000b).

The Nunnock River is a tributary to the Bemboka-Bega River, which drains into the Pacific Ocean at Bega (Fig. 1). The granite cliffs of the escarpment, downslope from the low-gradient headwaters region, and a relatively steep drop off the escarpment

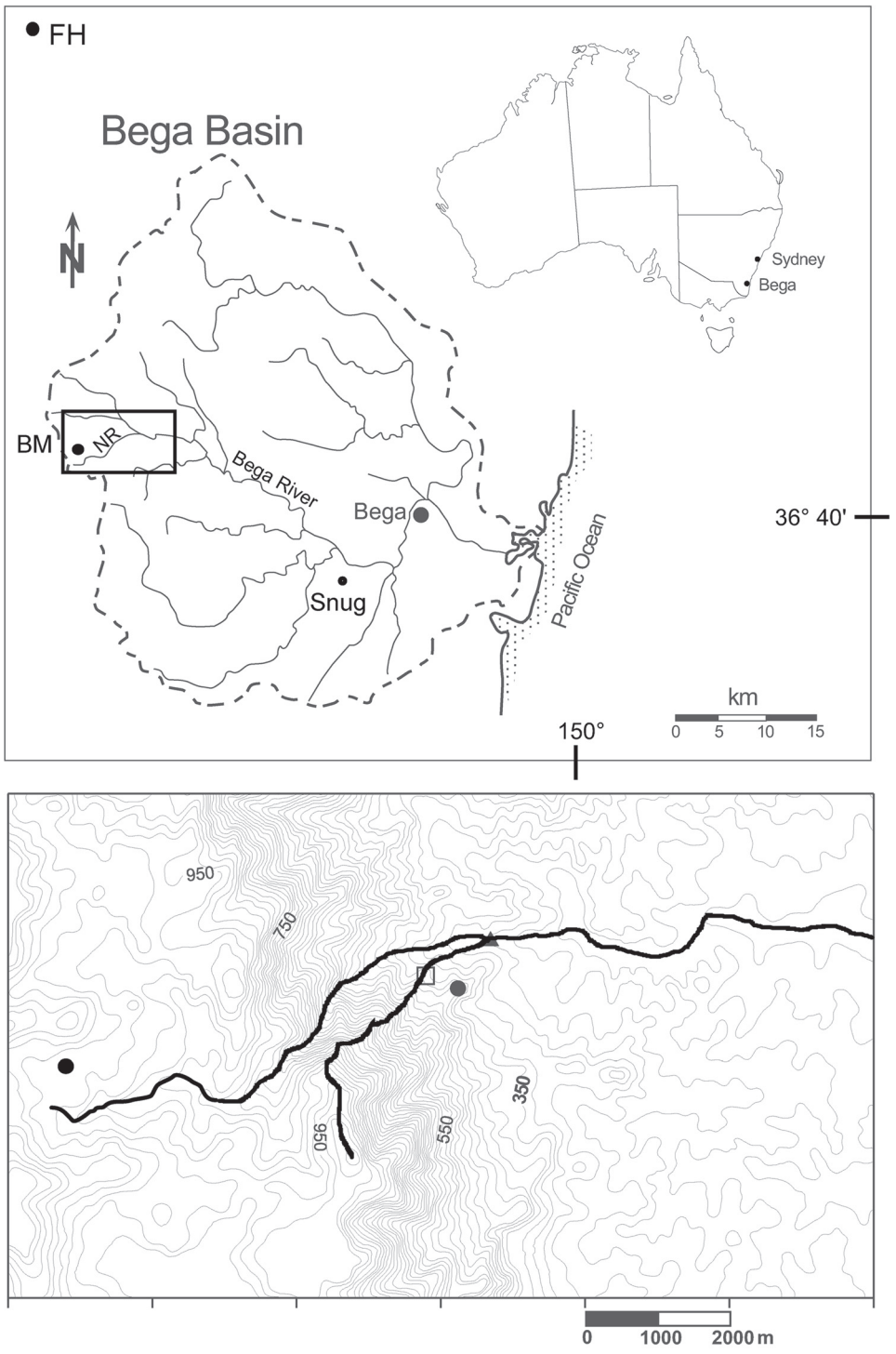

Figure 1. Location map showing the topography across the escarpment face. Outline of the Bega basin shown by dashed line, with Nunnock River shown by NR in the middle of the location rectangle. Topography of the lower panel is with 20 m contour intervals from 1:100,000 digital data (Australian Surveying and Land Information Group) from Bega (sheet 8824) map. Locations used for the Heimsath et al. (2000) study are shown by: black dot on ridge crest at base of escarpment is where Figure 2 photos were taken from; open square shows approximate location of the surveyed area of the Heimsath et al. (2000) study; and black triangle shows stream sediments from Nunnock River used in that study (modified from Heimsath et al., 2000). Approximate locations of the lowland (Snug) and two highland (Brown Mountain [BM] and Frogs Hollow [FH]) sites shown by black dots and labels on map, with the FH site ~20–30 km north of the shown region. Black lines across the escarpment topography show the profiles plotted in Figure 3A–B, where the channel line is extended farther here than in the profile data.

Figure 2. Photographs from the ridge crest tor location used to develop the tor erosion model presented in Heimsath et al. (2000). View is upslope showing the spur ridge used for elevation transect of this study (A), where the "V" visible on skyline is the incision of Nunnock River across the escarpment crest. Note tree cover of the escarpment and the relatively small region of exposed cliffs, directly above middle person's head, which is not visible from below. (B) View downslope to the Pacific Ocean, horizontal skyline roughly 50 km distant, shows drop of the higher-relief escarpment slopes to more gently sloping, lower-relief coastal lowlands.

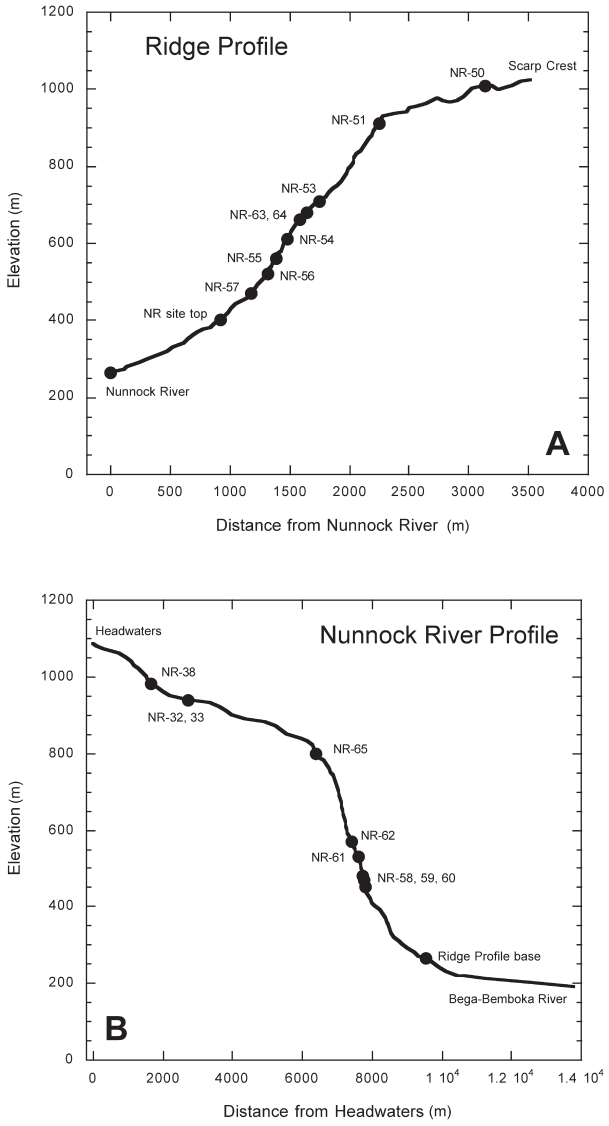

Figure 3. Elevation versus distance profiles for the spur ridge used to collect samples for this study (A), as well as the long profile of Nunnock River (NR) as it traverses the escarpment (B). Note vertical exaggeration for both figures and that the distance axes are not at the same scale for A and B. Data for both profiles collected by hand off the 1:20,000 regional maps using 10 m contour intervals. Ridge profile begins where the spur ridge intersects with Nunnock River, shows the top of the field site of Heimsath et al.'s (2000) study area, and marks sample elevations with the filled black circles. Corresponding sample ID numbers are noted adjacent the circles. Profile ends at the scarp crest. River profile begins in the low-gradient, swampy meadow headwaters of the Nunnock River at the farthest upslope extent of the channel. Catchment area at the channel head is approximately one hectare, and the landscape is soil-mantled, dotted with outcropping tors. Small catchment sediment sample average elevations are shown on the river profile with filled black circles and are marked with the sample ID numbers used in Table 1. Nunnock River changes from sand-bedded, relatively incised channel across the low-gradient highlands to a steeply dropping, bedrock river across the escarpment with obvious fluting and fluvial incision channels. Large boulder deposits are observed beginning near the escarpment base, but are not present in the Bega-Bemboka River.

define the drainage area of Nunnock River. Evidence of debris-flow deposits are found in each of the second-order drainages downslope from the escarpment, though scour to bedrock on the escarpment face is relatively limited. The exposed cliff region across the top of the escarpment is not as dramatic or extensive as those from the Weissel and Seidl (1998) study area, but they are eroding by block failure across their face and thin exfoliation sheet erosion across their tops. There is little sediment accumulation beneath the cliffs, and it appears that the upper region of the escarpment is weathering-limited, as are regions of the channels

(the channels are bedrock with the exception of patchy debris-flow cover). Spur ridges are soil-mantled and perpendicular to the escarpment. Slopes are sharply convex across the tops of the regions and steepen downslope to the channel (Heimsath et al., 2000). Between Nunnock River and the coastline, the landscape is composed of rolling, granodiorite hills with very few outcropping tors in comparison with the highland region. The granodiorites are Late Silurian to Early Devonian and are part of the Bega Batholith Igneous Suite (Lewis and Glen, 1995). Relief is <200 m across the coastal lowland and increases from the coast inland to the escarpment, which rises abruptly for ~800 m directly west of the scarp base field site.

Rainfall on the coastal lowlands (~900 mm/yr), and especially near the escarpment, is considerably higher than on the tablelands, though it does fall sporadically throughout the year (Richardson, 1976). Rainfall intensities are reportedly higher near the escarpment (personal commun. with landowners), though this has not been quantified beyond the past 10 yr. Using stations of the Australian Bureau of Meteorology (www.bom.gov.au/climate/averages) closest to the field sites, the average rainfall ranges from 870 mm/yr for the coastal lowland site (Snug, at ~200 m elevation), to over 1200 mm/yr at the escarpment base (Nunnock River, at 400 m), to 690 mm/yr at the escarpment crest (Brown Mountain, at 1000 m), to 720 mm/yr at the highland site (Frogs Hollow, at 900 m). Observed vegetation at the escarpment base reflects this higher rainfall compared with the relatively dry and cold tablelands region, and forest cover is intermediate to wet schlerophyll forest with patches of dense understory, especially in the valley bottoms. Ferns grow widely on the more humid slopes around the Nunnock River field area, but are not observed on the slopes nearer the coast at the Snug site.

The field area of Heimsath et al. (2001) is representative of the low-relief plateau of the highlands above the escarpment, but is northwest of the Nunnock River portion of the escarpment leading to the coastal lowlands focused on here, motivating sampling another highland area around Brown Mountain. This highland site is the same region studied by Banfield and Eggleton (1989) and Taunton et al. (2000a, 2000b). The highlands, in general, are between ~800 and 1500 m above sea level. Bedrock varies between Ordovician metasediments and Devonian granites across the region (Richardson, 1976). Morphology of the highlands directly above the Nunnock River site (i.e., Brown Mountain) is similar and is characterized by low-relief hillslopes (<100 m) that are gently sloping (<25°) and are soil-mantled, but punctuated frequently by tors. These tors are typical examples of the more coherent bedrock that outcrops through a saprolitic granite landscape (e.g., Linton, 1955; Twidale, 1985; Williams et al., 1986). The weathered nature of the soil-mantled saprolite is exposed in numerous road cuts around the field areas. These road cuts also reveal the prevalence of core-stones, some fraction of which are likely to emerge sometime in the future as tors.

The climate of the southeastern highlands is relatively cool, averaging ~18–22 °C in the summer and 3–5 °C in the winter. There are periods of freezing temperatures and snow in the winter, but these rarely last long. Rainfall is not distinctly seasonal and, with the exception of drought periods, does not vary much from ~550–750 mm/yr (McAlpine and Yapp, 1969; Richardson, 1976). Forest cover, where it occurs, is typically dry schlerophyll, with very little understory. Grassland and rolling savanna woodland vegetation are also widespread across this region of the tablelands. Climate changes during the Pleistocene and during the Pleistocene–Holocene transition (Bryant et al., 1994; Chappell, 1991; Dodson, 1977, 1987; Dodson and Wright, 1989; Harrison, 1993; Kershaw et al., 1991) probably affected the biotic communities and therefore the dominant soil production and transport processes. These processes were likely similar to the Nunnock River site since the biota are similar, but the drier and colder climate may reduce the frequency of the bioturbation at the highland sites. Potential impacts of historic agriculture were avoided by selecting protected areas for our work.

Soil production and transport is observed to be primarily due to biogenic processes across all field areas, although there is some evidence of overland flow, especially during storms following fires that remove any vegetative understory. Burrowing wombats were the most obviously disruptive biota and were observed to occupy all parts of the landscape except where soil thickness was less than ~30 cm, and their burrows extend into the weathered bedrock in places. Other observed biogenic processes included burrowing echidnas and shallow burrowing lyre-birds, worms (worm trails extended into the saprolite and worm castings in the soil included quartz crystals that could have been conveyed up from the underlying saprolite), and tree throw (Fig. 4). Ant or termite mounds revealed significant quartz grains and pieces of unweathered granodiorite, but we did not observe ant burrows extending into the saprolite; therefore, we infer that such microfauna contribute to transport rather than production of the soil.

METHODS

In situ–produced cosmogenic nuclides (e.g., ^{10}Be and ^{26}Al) are used increasingly to quantify bedrock erosion (e.g., Lal, 1991; Nishiizumi et al., 1991), soil production (e.g., Heimsath et al., 1997; Small et al., 1999), and spatially averaged rates of erosion (e.g., Bierman and Steig, 1996; Brown et al., 1995; Granger et al., 1996). Concentrations of these nuclides accumulate in materials at or near Earth's surface as cosmic rays bombard atoms, such as Si and O in quartz and other minerals in rock and sediments (Lal and Arnold, 1985; Lal and Peters, 1967). Cosmic-ray production of nuclides is balanced by radioactive decay of the nuclides in surfaces that are not eroding and by removal of the target material in eroding surfaces. Application of cosmogenic nuclide analysis to understanding landscapes is extensively and well-reviewed (Bierman, 1994; Cockburn and Summerfield, 2004; Gosse and Phillips, 2001; Lal, 1988; Nishiizumi et al., 1993) and will only be summarized here.

Nuclide concentrations measured from quartz have been shown to reflect the exposure history of the sample and are dependent on the production and decay rates of the nuclide, as well as

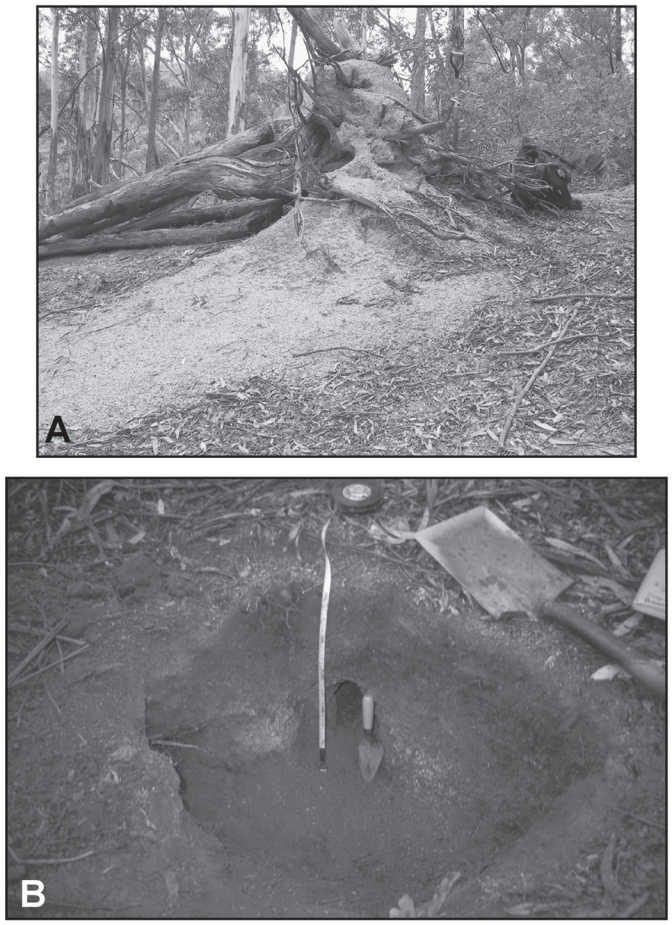

Figure 4. Photos showing the more dramatic of the biogenic processes acting across each of the field areas. Tree throw of the *Eucalyptus* sp. is common and typically shows uprooted granitic saprolite clinging to the roots (A). Here the fan-shaped, light-colored deposit from the uprooted tree was observed to be primarily quartz grains from the saprolite, which were penetrated by the roots prior to uprooting. Wombat burrows (B) commonly penetrate the saprolite, such that the downslope deposits from the burrows are mixtures of saprolite and soil, similar to the observations of gopher burrowing by Gabet (2000). Tape measure for scale shows burrow diameter to be ~30 cm, with the trowel handle at the approximate location of the soil-saprolite interface.

the erosion rate of the sample (Lal, 1988; Lal and Arnold, 1985; Nishiizumi et al., 1986, 1991). As shown by Lal (1991), and neglecting muon effects, the nuclide concentration, C, depends on the production of the nuclide at an exponential depth, z_x, function of the surface production rate, P_0, and its radioactive decay constant, λ,

$$\frac{dC}{dt} = P_0 e^{-\mu z_x} - \lambda C, \qquad (1)$$

where μ is the absorption coefficient (equal to material density divided by the mean attenuation length for cosmic rays, Λ, where $\Lambda \sim 165$ g cm^{-2}), and $\lambda = \ln 2/t_{1/2}$, where $t_{1/2} = 1.5 \times 10^6$ yr for ^{10}Be and $t_{1/2} = 7.01 \times 10^5$ yr for ^{26}Al). If erosion, ε, is assumed, based on geomorphic examination, to be constant over the exposure history of the sample, equation 1 can be solved analytically (Lal, 1991), yielding,

$$C = c_0 e^{-\lambda t} + P(H,\theta)\left(\frac{1}{\lambda + \mu\varepsilon}\right) \qquad (2)$$

at secular equilibrium, when $t >> (\lambda + \mu\varepsilon)^{-1}$, where $P(H, \theta)$ is the nuclide production rate (atom g^{-1}yr^{-1}) at the soil-bedrock boundary under slope-normal soil depth, H, and on a surface with slope θ, and C_0 is the initial concentration of the nuclide. $P(H, \theta)$ is calculated as a factor of the surface nuclide production rates (e.g., Dunne et al., 1999). Under steady-state conditions, where local soil thickness is relatively constant with time, soil production, ε_s, equals erosion, ε, at the surface, which is also equal to the rate of lowering of the soil-saprolite interface (Heimsath et al., 1997) and can therefore be equated to the local denudation rate. Equation 2 can therefore be solved to yield steady-state soil production or erosion rates. Nuclide concentration accumulated in river or catchment sediments can be interpreted by equation 2 to infer catchment-averaged steady-state erosion rates, assuming relatively short transport times and relatively homogeneous catchment lithology (e.g., Granger et al., 1996; Bierman and Steig, 1996).

We apply this methodology to determine erosion rates in three different ways. Most simply, we sample the outermost centimeter or two of exposed bedrock (tor tops as well as the top of the cliff region of the escarpment) that shows field evidence of eroding by grain-grain spallation or by exfoliation of thin sheets. Concentrations of ^{10}Be and ^{26}Al in these samples yield the inferred steady-state erosion rate of the exposed bedrock surfaces, assuming that samples have had simple exposure histories (e.g., no significant burial or shielding that is now not evident) and have been eroding at nearly constant rates (i.e., not by large block failure or landsliding). For soil production rate determination, we followed the typical geomorphic transect from bedrock exposed at convex ridge crests onto the soil-mantled part of the landscape and dug soil pits to sample the top centimeter or two of saprolite or weathered bedrock directly beneath different depths of the relatively thin (<1 m) soil cover. Concentrations of nuclides from these samples were used with a corrected nuclide production rate that accounts for the shielding of the soil mantle above the sampled layer to yield a soil production rate, which is equivalent to a landscape-lowering rate relative to a local datum (Heimsath et al., 1999). Finally, we collected stream and creek sediments or sediment from zero-order catchments, measured the concentrations of the nuclides, and used the nuclide concentrations to infer a catchment-averaged erosion rate (e.g., Granger et al., 1996). Each of these applications depends on careful geomorphic site selection, such that the numerous assumptions and simplifications detailed in the above studies are met.

Roughly 500 g of bedrock, saprolite, or sediment from each sample were crushed, sieved to separate particles <1 mm size, and chemically purified following the procedure of Kohl and Nishiizumi (1992) to yield ~50 g of quartz, from which Be and Al were

extracted. For results reported here we only measure concentrations of ^{10}Be, because sample lithology and exposure history were similar to those reported in Heimsath et al. (2000, 2001) and did not warrant the test for steady-state exposure history enabled by measuring ^{26}Al (e.g., Nishiizumi et al., 1993). Samples for ^{10}Be measurement were spiked with a ^{9}Be carrier solution calibrated by a Be atomic absorption standard that differed by <2% from the Be carrier used for the Nishiizumi et al. (1989) analyses. Preparation and chemistry on these samples were done at Dartmouth College as well as at the Research School of Earth Sciences at the Australian National University (ANU). We measured concentrations of ^{10}Be at the Lawrence Livermore National Laboratory, Center for Accelerator Mass Spectrometry (LLNL-CAMS) facility (Davis et al., 1990) as well as at the ANU Nuclear Physics facility and Purdue University's PRIME Lab, and standardized the measurements to the ICN (ICN Biomedical, Inc.) ^{10}Be standards. By doing the chemistry on these samples in two very different labs and measuring the nuclide concentrations on three very different accelerator mass spectrometers, we also have an excellent test for the potential analytical uncertainties in the cosmogenic nuclide methodology used for geomorphic studies.

Production rates for ^{10}Be and ^{26}Al in quartz were based on the sea-level and high-latitude production rates of 6 and 36.8 atoms g^{-1} yr^{-1} (Nishiizumi et al., 1989), rescaled to 5.1 and 31.1 atoms g^{-1} yr^{-1}, respectively (Stone, 2000), and were corrected for latitude and altitude effects (Lal, 1991), as well as for the slope and shielding of the sample (Dunne et al., 1999; Masarik and Vanya, 2000; Nishiizumi et al., 1989). These production rates were used for consistency with previous reports of erosion rates or exposure ages, despite the growing debate over production rates (Clark et al., 1995; Dunai, 2000; Nishiizumi et al., 1996; Stone et al., 1998a) and the potential contribution of muons to nuclide concentrations under moderate and high erosion rates (e.g., Granger and Smith, 2000; Stone et al., 1998b).

RESULTS AND DISCUSSION

The Highlands

Results from the new nuclide analyses are reported here for ^{10}Be concentrations, with the erosion rates or soil production rates determined from them (Table 1). Table 1 does not distinguish between samples prepared at different laboratories or measurements made at different accelerators. The results presented below incorporate these differences and agree so well that we believe the soundness of our methodology is maintained. Seven samples from directly beneath the actively eroding soil mantle define a soil production function for the highland landscape at Brown Mountain (Fig. 5A). Two samples from bedrock exposed at the soil surface yield steady-state erosion rates and suggest that maximum soil production rates occur under some finite soil mantle (Ahnert, 1987; Carson and Kirkby, 1972; Dietrich et al., 1995; Gilbert, 1877), such that the soil production function could have a "humped" form (Cox, 1980). Measured nuclide concentrations were corrected for observed soil depths (Heimsath et al., 1999), and steady-state erosion rates, calculated with equation 2, define an exponential decline of apparent soil production rates with increasing soil depths for the saprolite samples. The variance-weighted best fit to these points, excluding the bedrock points, is

$$\varepsilon(H) = 65 \pm 15 e^{-(0.020 \pm 0.003) H}, \quad (3)$$

where the soil production rate, $\varepsilon(H)$, is the vertical lowering rate in Table 1 in m/m.y., and H is in cm. Comparison of these data with the soil production and exposed bedrock erosion rates reported for the highland site of Heimsath et al. (2001) shows remarkable similarity in rates and form despite the sites being nearly 60 km apart and the samples being collected and analyzed about four years later in a different laboratory (Heimsath et al., 2001, analyses were done at the University of California, Berkeley; Fig. 5B). The apparent soil production function reported by Heimsath et al. (2001) was fit to five samples using both ^{10}Be and ^{26}Al from beneath soil thicknesses from 25 to 65 cm and had a dramatically steeper slope to it, such that the function defined an intercept that was unreasonably high for any rates measured across the highlands:

$$\varepsilon(H) = 143 \pm 20 e^{-(0.042 \pm 0.003) H}. \quad (4)$$

Arguably, the combined soil production data from the highland sites (Fig. 5B) would define a humped soil production function, as first articulated by Carson and Kirkby (1972) and also discussed by Cox (1980). This is discussed below, after presentation of all the soil production data.

Similarities in morphology between the two highlands sites suggest that the conclusions reached by Heimsath et al. (2001) are applicable to the escarpment crest region. Specifically, that extensive outcropping tors are found at both sites and that the weathering profiles visible in the road cuts, and analyzed at a site very close to our Brown Mountain site by Banfield and Eggleton (1989) and Taunton et al. (2000a, 2000b), support the notion of a propagating weathering front into the relatively stable highlands. Their measurements suggest considerable erosion by solute processes, while our cosmogenic nuclide–determined lowering rates are recording a total lowering rate with no differentiation between chemical and physical weathering processes. It is clear from the weathering profiles that solute processes are significant, and it is also clear from the active bioturbation across the landscape that physical soil production and transport are significant. At this point, we cannot resolve the relative roles that both play, though it is clear that they are coupled as Riebe et al. (2001, 2003) found elsewhere, and we are examining the problem with a detailed look at how the extent and rate of weathering varies across the landscape (Burke and Heimsath, 2003).

Average erosion rates from ^{10}Be concentrations from stream sediments taken from small catchments draining to Nunnock River above the escarpment range from 13 ± 1.7 to 20 ± 2.5 m/m.y.

TABLE 1. EROSION RATES FROM COSMOGENIC NUCLIDE CONCENTRATIONS

Sample	Depth[†] (cm)	Type[‡]	PROD. factor[§]	Elev. (m)	Wt. (g)	Be (mg)	^{10}Be 10^6 atoms/g	±	ε (m/m.y.)	±	% error
Cosmogenic nuclide concentrations from small catchment sediments											
NR-32		Avg	0.9	940	20.89	0.451	0.258	0.012	15.47	1.50	9.7
NR-33		Avg	0.9	940	19.40	0.447	0.251	0.012	15.88	1.55	9.8
NR-38		Avg	1.0	980	21.04	0.434	0.307	0.023	13.43	1.69	12.6
NR-58		Avg	0.9	450	48.79	0.455	0.153	0.011	27.79	3.42	12.3
NR-60		Avg	0.6	478	51.30	0.524	0.082	0.004	29.20	3.04	10.4
NR-61		Avg	0.6	525	47.69	0.542	0.064	0.007	35.87	5.64	15.7
NR-62		Avg	1.2	570	25.89	0.513	0.175	0.011	27.12	3.02	11.1
NR-65		Avg	0.4	800	48.86	0.489	0.092	0.007	20.13	2.51	12.5
Cosmogenic nuclide concentrations from brown mt. saprolites											
NR-34	60	BM	1.5	950	19.80	0.437	0.354	0.056	18.08	4.68	25.9
NR-36	0	BM	1.2	950	22.12	0.445	0.213	0.019	22.21	3.11	14.0
NR-37	25	BM	1.4	965	20.30	0.441	0.186	0.021	31.65	6.77	21.4
NR-39	55	BM	1.0	970	22.38	0.442	0.250	0.020	16.70	2.99	17.9
NR-41	50	BM	0.9	1033	21.24	0.435	0.149	0.018	26.59	5.87	22.1
NR-42	100	BM	0.4	1033	20.33	0.436	0.192	0.016	6.23	1.15	18.4
NR-43	70	BM	0.7	1066	21.69	0.435	0.195	0.024	16.05	3.58	22.3
NR-45	73	BM	0.8	1091	21.32	0.438	0.519	0.052	6.79	1.37	20.1
NR-50		Rdg	1.3	1015	23.70	0.443	0.400	0.017	12.44	1.15	9.2
Cosmogenic nuclide concentrations from ridge crest samples											
NR-51		Rdg	1.0	912	20.98	0.443	0.241	0.012	16.20	1.58	9.8
NR-53		Rdg	1.4	710	22.12	0.445	0.212	0.010	20.84	2.01	9.6
NR-54		Rdg	0.7	606	20.30	0.441	0.078	0.012	32.90	6.60	20.0
NR-55		Rdg	0.6	566	21.04	0.434	0.085	0.005	31.00	3.50	11.3
NR-56		Rdg	0.7	517	22.38	0.442	0.089	0.006	33.56	3.96	11.8
NR-57		Rdg	1.1	468	19.79	0.440	0.110	0.009	36.27	4.76	13.1
NR-59		Rdg	1.1	470	34.68	0.530	0.108	0.011	32.67	5.01	15.3
NR-63		Rdg	1.4	660	49.21	0.508	0.206	0.009	25.33	2.43	9.6
NR-64		Rdg	1.3	680	48.82	0.499	0.210	0.011	19.95	2.03	10.2
Cosmogenic nuclide concentrations from tor samples											
NR-30		Tor	2.0	1125	23.70	0.443	1.963	0.071	3.26	0.28	8.6
NR-31		Tor	2.0	1125	20.98	0.443	1.692	0.064	3.78	0.33	8.8
NR-35		Tor	1.8	950	23.90	0.442	0.396	0.018	14.19	1.35	9.5
NR-40		Tor	1.9	1033	19.79	0.440	0.317	0.021	18.80	2.16	11.5
NR-44		Tor	1.9	1071	20.46	0.438	1.470	0.072	4.18	0.41	9.9
NR-52		Tor	1.5	819	23.90	0.442	0.245	0.010	20.01	1.83	9.1
Cosmogenic nuclide concentrations from lowland site, SNUG											
NR-101	85	Snug	1.2	212	31.88	0.453	0.090	0.020	11.13	2.66	23.9
NR-102	27	Snug	1.1	214	31.15	0.456	0.1	0.01	24.51	2.50	10.2
NR-103	70	Snug	1.1	215	30.24	0.391	0.1	0.1	9.75	1.30	13.3
NR-104	90	Snug	1.1	216	31.28	0.325	0.13	0.02	9.48	1.53	16.2
NR-105	70	Snug	1.2	217	30.61	0.370	0.21	0.04	4.19	0.88	21.0
NR-106	45	Snug	1.1	220	30.94	0.456	0.16	0.01	11.43	0.73	6.4
NR-107	38	Snug	1.2	221	30.20	0.454	0.12	0.01	17.27	1.47	8.5
NR-108	60	Snug	1.2	222	29.63	0.359	0.13	0.01	11.30	0.89	7.9
NR-109	50	Snug	1.1	223	30.67	0.406	0.03	0.02	57.38	6.92	12.1
NR-110	70	Snug	1.2	227	29.68	0.368	0.177	0.027	7.01	1.13	16.2
NR-111	0	Snug	1.1	228	29.97	0.377	0.421	0.081	8.72	1.79	20.6

Note: All errors are propagated to soil production or erosion rate, ε.

[†]Average soil density: 1.2 g/cm^2.

[‡]Avg are catchment averaged, Rdg are Spur ridge crests.

[§]Production factor scales nuclide production for slope, soil depth, elevation, and latitude. Location of site at escarpment base: 36.62 S Lat, 149.5 E Long. ^{26}Al and ^{10}Be concentrations scaled from sea-level production rates of 36.8 and 6 atoms g^{-1} yr^{-1}.

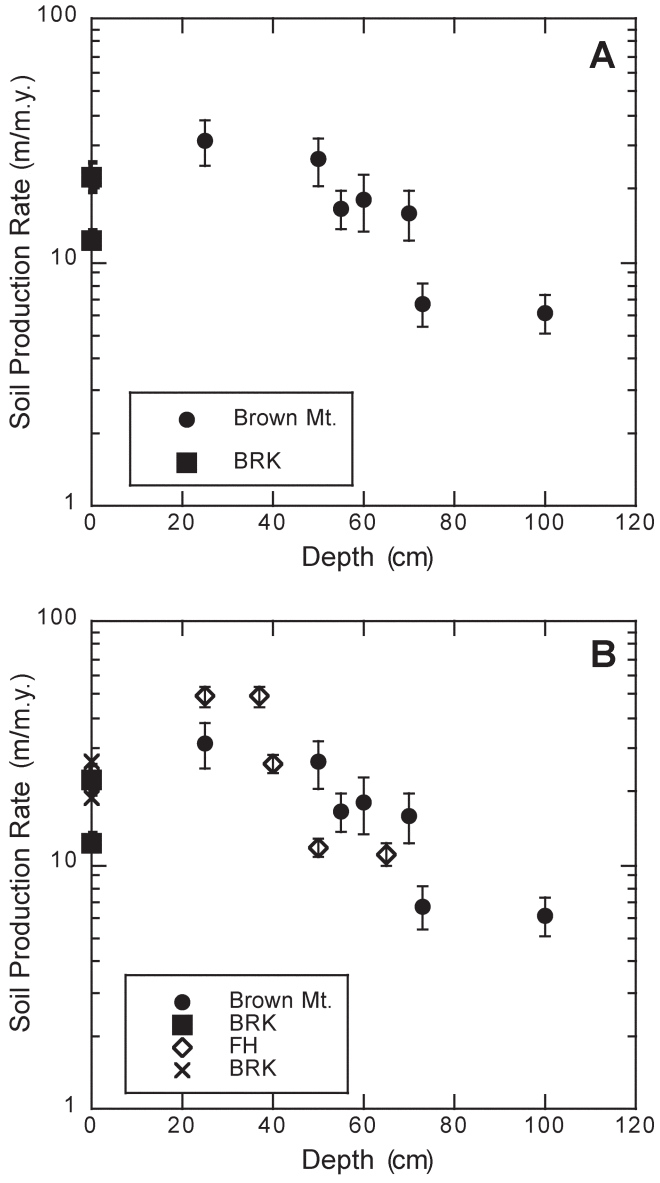

Figure 5. Soil production (m/m.y.) plotted as a function of overlying soil depth (cm). Solid black circles in A are rates derived from ^{10}Be concentrations (Table 1) in samples from the highland site near Brown Mountain (BM), and error bars represent all errors propagated through the nuclide calculations, i.e., uncertainty in Be carrier concentrations, accelerator mass spectrometry, bulk densities, and soil depth measurements, and attenuation length of cosmic rays. See text equation 3 for variance-weighted best fit to the soil production data. Black squares plotted at zero depth are erosion rates of bedrock (BRK) exposed at ground surface. Comparison with the soil production and bedrock erosion rates reported in Heimsath et al. (2001) from both ^{10}Be and ^{26}Al is shown in B, where the open diamonds are soil production rates and crosses at zero depth are exposed bedrock samples at the ground surface from that site, Frogs Hollow (FH). See text equation 4 for the soil production function from Frogs Hollow.

(Table 1; Fig. 3B). These rates are at the low end of the escarpment erosion rates discussed below, but agree well the highland soil production rates shown in Figures 5A and 5B. This is encouraging support for the use of small catchment sediments to quantify average erosion rates for a landscape, as the processes of soil production and transport are the dominant geomorphic forces shaping the highlands. Landslides and extensive gullying are only observed where there is a clear link between overgrazing by livestock and local degradation of the land surface following increases in rainfall. Tor erosion rates are slower, as discussed in Heimsath et al. (2000, 2001), and by quantifying the sediment budget for the catchment, the interpretation of the nuclide concentrations in the sediment samples reflects well the proportional contributions of tor erosion and soil production from the saprolite (Granger et al., 2001; Heimsath et al., 2001). The overlap between average and point specific rates supports the suggestion that the highlands may have reached a steady-state since emerging from the last glacial cycle, when periglacial processes were likely to be dominant, a suggestion that was raised in the "Departures from Steady State: (II) Soil Production" section of Heimsath et al. (2001, p. 180–181).

The Lowlands

Ten samples from the saprolite-soil boundary at the coastal lowland site (Snug) define soil production rates for soil depths between 27 and 90 cm (Fig. 6A). No intermediate soil depths were observed, and the sample from bedrock exposed at the soil surface led to a lower soil production rate than the sample from beneath the shallowest soil, a finding similar to the highland sites. Analyses of the nuclide concentrations followed procedures outlined above, correcting for overlying soil thickness to infer steady-state soil production rates. Using the saprolite soil production rates to determine a variance-weighted best fit for the soil production function, we determine that,

$$\varepsilon(H) = 42 \pm 5e^{-(0.020\pm0.002)H}, \quad (5)$$

where the variables are the same as defined previously. With the exception of sample NR-109, which determined an especially high soil production rate and is likely to be an outlier due to local disturbance of the long-term average soil thickness (i.e., if soil thickness had been locally stripped, due to anthropogenic activity or local burrowing, then the long-term nuclide production rates would not be correctly scaled for depth and the inferred soil production rate would be anomalously high), the Snug data complement and extend the function defined at the base of the escarpment (Nunnock River) by Heimsath et al. (2000). The notable difference between the Snug and Nunnock River sites was the absence of intermediate soil thicknesses, and further investigation is required to decided whether this is true across the coastal lowland region, as we observe it to be for the highlands, or if there is the potential for human impact that may have left a plow layer. A plow layer is a surficial layer of soils with

near-uniform thickness that would be present if any plowing of the site had homogenized soils down to a finite depth, typically ~30 cm. The soil production function defined from Nunnock River, at the base of the escarpment, was from both ^{10}Be and ^{26}Al concentrations measured in 15 samples of saprolite and bedrock and showed the following very well-defined exponential decline of soil production rates with increasing soil thicknesses (Heimsath et al., 2000):

$$\varepsilon(H) = 53 \pm 3e^{-(0.020\pm0.001)H}. \quad (6)$$

Plotting the two data sets together shows nearly identical relationships despite the offset of the intercept between the two functions (Fig. 6B). This overlap is surprising, as the coastal lowlands have lower relief and are more gently sloping than the soil-mantled slopes adjacent to the escarpment base. Conventional wisdom would suggest that the lowlands and highlands would be eroding more slowly than the escarpment base, yet our cosmogenic nuclide data suggest otherwise.

If we plot soil production rates from all four of the field sites from lowland to highland, the overlap becomes especially clear (Fig. 7). Indeed, using all these data, again with the exception of the exposed bedrock samples that are eroding more slowly (discussed below), to determine a variance-weighted soil production function tightens the relationship of equation 6 such that

$$\varepsilon(H) = 53 \pm 2e^{-(0.022\pm0.001)H}. \quad (7)$$

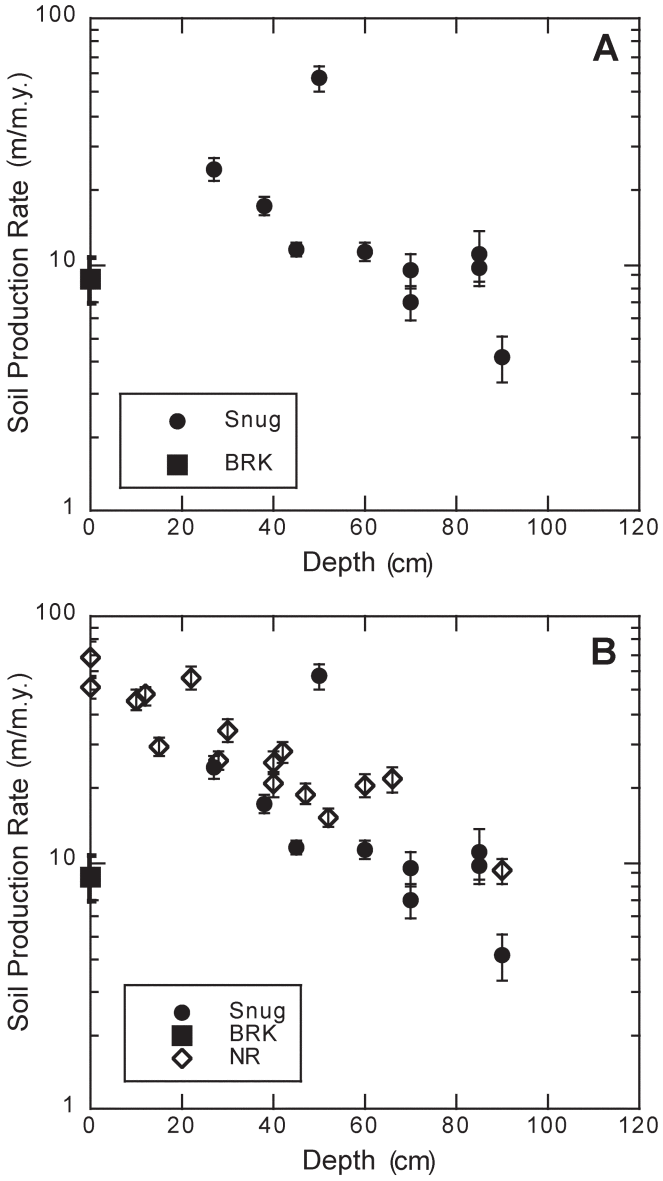

Figure 6. Soil production (m/m.y.), plotted as a function of overlying soil depth (cm). Solid black circles in A are rates derived from ^{10}Be concentrations (Table 1) in samples from the lowland site (Snug) between the Nunnock River (NR) site of Heimsath et al. (2000) and the town of Bega. Comparison with the soil production function reported in Heimsath et al. (2000) from both ^{10}Be and ^{26}Al is shown in B, where the open diamonds are from Nunnock River. Calculation details are the same as above; see text equation 5 for the variance-weighted best fit to the soil production data of A, while the fit to the Nunnock River data is in the text as equation 6. BRK—bedrock.

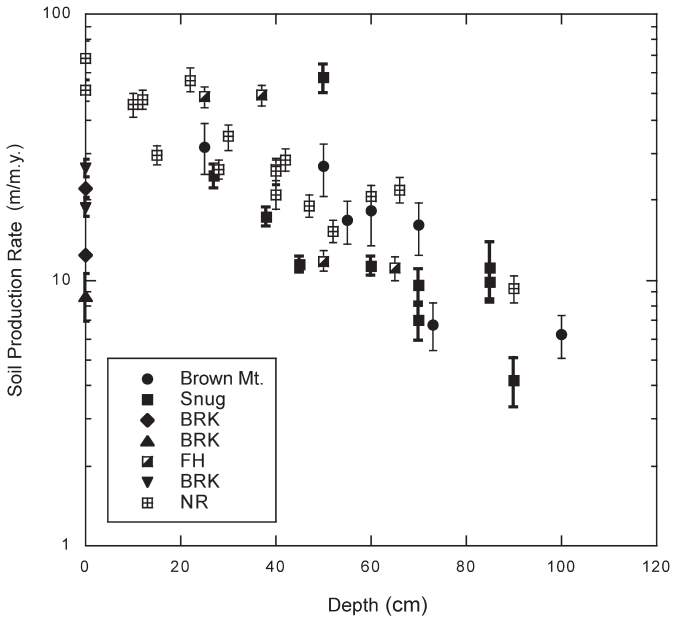

Figure 7. Soil production rates plotted for all four field sites discussed here. The two new sites, Brown Mountain and Snug, are the same data as Figures 5A and 6A, respectively, while the data from the Heimsath et al. (2000, 2001) studies are the same as plotted with Brown Mountain and Snug data in Figures 5B and 6B, respectively. Erosion rates of bedrock exposed (BRK) at the soil surface are plotted for all sites with different symbols. Variance-weighted best fit to all the soil production data plotted here is reported in the text as equation 7. NR—Nunnock River; FH— Frogs Hollow.

That landscapes with such different climates and tectonic histories show such similar soil production functions is surprising, but may support the notion of a rapid achievement of steady-state to current conditions. If biota are the dominant force in producing and transporting soil, then the differences between the sites are not dramatic. All sites have burrowing organisms, trees, and receive roughly similar rainfall rates, though there is a nearly twofold decrease in precipitation with elevation, as documented in the site descriptions. Frost conditions have not been quantified, but are likely to be minimal on the highland sites, as temperatures below freezing are not common.

That exposed bedrock at the highland and lowland sites appears to be eroding more slowly than the maximum soil production rates determined under relatively thin depths of soil raises an important distinction between soil production functions (Carson and Kirkby, 1972; Cox, 1980; Dietrich et al., 1995). Specifically, if lithology is uniform beneath the actively eroding soil layer, then lower rates of erosion for exposed bedrock document the hypothesis articulated by Gilbert (1877) from his observations that weathering processes attributed to frost and solute processes would occur most rapidly beneath a thin soil cover. A thin soil cover would enable moisture retention at the soil-rock interface, such that chemical and physical weathering processes could occur. Dietrich et al.'s (1995) modeling yielded an unreasonable modeling prediction of the spatial variation of soil thickness using such a humped soil production function. Specifically, they used both humped and exponentially declining soil production functions in a model predicting spatial patterns of soil thickness at the same soil-mantled field site in northern California, which was used subsequently by Heimsath et al. (1997, 1999). Using the humped function predicted widespread bedrock exposure not observed in the field, while using the exponential decline predicted soil depths consistent with observations. Carson and Kirkby (1972) explained that having maximum soil production rates beneath a finite soil thickness would lead to landscapes with either exposed bedrock, or soil thicknesses greater than the finite depth, with no intermediate soil depths. This suggestion was documented for the highland site of Heimsath et al. (2001), where modeling spatial variation of soil depth led to a better prediction of soil thickness when the exponential decline function was used, and Small et al. (1999) presented similar findings for an alpine landscape. Ahnert's (1987) modeling presented a different perspective, which was that variations in the underlying bedrock could lead to soil depth variations across a hypothetical landscape eroding at the same rate everywhere. Importantly, variations in lithology documented at the highland site may help to explain why the soil production functions from the highlands and lowlands are different from those presented from the escarpment base and northern California (Heimsath et al., 1997, 1999), emphasizing the importance of knowing the chemical weathering story by quantifying both the extents and rates of chemical weathering across all sites following, for example, methods of Riebe et al. (2001, 2003).

Across the Escarpment

Eight samples define catchment-averaged erosion rates from small, first- and zero-ordered streams draining the escarpment to Nunnock River, while ten samples from a main spur ridge define point-specific erosion rates for an altitudinal transect along a main spur ridge from coastal lowland to the Brown Mountain site (BM; Table 1). We include tops of three granite tors from the escarpment crest, near Brown Mountain, as well as three samples from the tops of outcropping granite faces along the steep escarpment face, where the only cliff exposures are found for this region of the escarpment (plotted as Tor Top). Together these 24 samples, along with average soil production rates from the scarp base site and the lowland site (plotted as separate ridge crest points), yield a striking trend of erosion rates as a function of elevation (Fig. 8), from 3.26 ± 0.28 m/m.y. at the scarp crest to an apparent peak of 36.3 ± 4.8 m/m.y. near the scarp base and declining to 24.5 ± 2.5 m/m.y. across the coastal lowlands. Local agreement between the rates determined for different processes

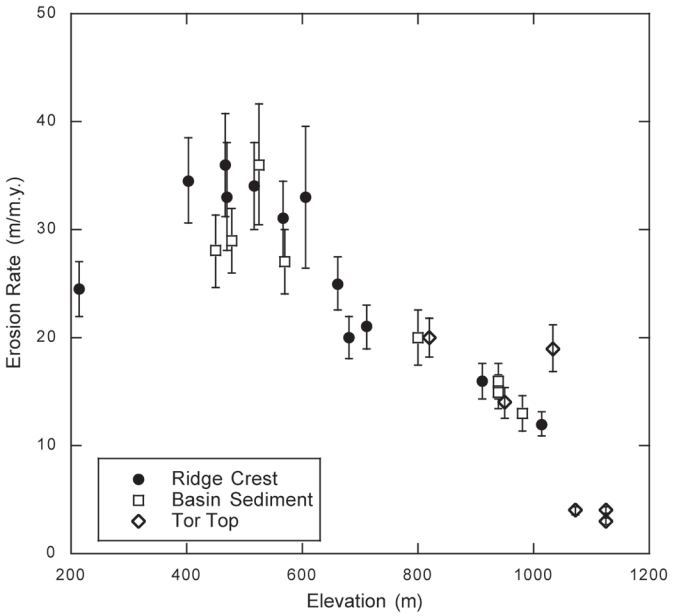

Figure 8. Erosion rate data from the ridge crest (filled black circles), small catchment averages (open squares), and tor tops (open diamonds) plotted as a function of elevation across the escarpment face. For most of the samples, the ridge crest and small catchment samples were adjacent and relatively nearby (within one to two hundred meters) for similar elevations. Ridge crest samples were from a single spur ridge leading directly up the escarpment from the study area of Heimsath et al. (2000), except for the NR-50 sample at 1015 m, which was from the ridge crest draining to the highest elevation small catchment sample, NR-38, with an average elevation of 980 m. The three tor tops from the highest elevation are from ridge crests draining to and near the headwaters of Nunnock River, while the tor top at 1033 m is from the top of a small granite cliff near the escarpment lip. Average values for the soil production rates at the scarp base (NR) and the coastal lowland (Snug) sites are included as additional two ridge crest samples.

suggests local steady-state between soil production, bedrock erosion, and small channel incision.

There are at least two mechanistic reasons to predict this order of magnitude decline in erosion rates, which are not entirely intuitive, because conventional wisdom might suggest increases in erosion rate with elevation. Firstly, observations that precipitation decreases with elevation across this escarpment would help explain the decline in erosion rates with elevation if there were a clear process link. At this stage we can simply suggest that higher precipitation at the escarpment base may support higher densities of biota, which are, in turn, likely to be more active across the landscape, potentially leading to higher erosion rates. While this suggestion is extremely speculative and needs field testing, it is critical that a process-based explanation be determined. Interestingly, the order of magnitude decrease of denudation with a <1000 m rise in elevation reported here is nearly the opposite of the less than a factor of 1.4 difference in rates reported by Riebe et al. (2004) across a <700 m altitudinal transect used as a steep climatic gradient in the Santa Rosa Mountains of Nevada. Their observations suggest a sharp decline in chemical weathering with altitude by coupling precipitation with total denudation, which may play a role here. We are currently testing this hypothesis. Secondly, both increasing stream power with distance downslope and increasing relief at the escarpment base would predict higher erosion rates with lower elevations across our field areas. Morphometrically, the correlation shown in Figure 8 fits with the low relief and gently convex-up ridges near and upslope of the scarp crest, as well as across the coastal lowlands, in comparison with the much higher relief and sharply convex ridge crests downslope on the scarp and onto the escarpment base site of Heimsath et al. (2000; see inset topographic map of Fig. 1). That is, lower erosion rates would be expected at the top of the escarpment and out on the coastal lowland based on the morphology, which is what the data show (note Fig. 6A, the soil production and bedrock erosion rates from Snug at an elevation of just over 200 m). The highest rates shown by Figure 8 are from the sharply convex-up ridge crest across and just upslope of the Heimsath et al. (2000) study area and from small catchments draining that ridge. Local relief, i.e., elevation difference between main spur ridge and the second- and third-order tributary draining the escarpment to Nunnock River, is greater at these sample sites than it is anywhere else on the escarpment, on the order of 50–60 m, and we observed debris-flow deposits in the main tributaries.

Increases in both slope and drainage area (a proxy for discharge) to the main tributaries draining the escarpment, of which Nunnock River is one example, with distance from the headwaters would predict the highest stream incision rates near the base of the escarpment. While the higher relief and over-steepened slopes adjacent to the streams at lower elevations at the escarpment base would suggest that stream incision rates are greater than ridge crest lowering rates, the lower elevation samples plotted in Figure 8 show similarity between the rates, within error. Importantly, the open boxes are average rates of first- and zero-order catchments draining from the spur ridges into the main tributaries, and are therefore not measures of the incision of Nunnock River or of the other main incision dissecting tributaries. We specifically chose the small catchments to avoid input of sediments or bedrock eroded by debris flows or landslides, such that the nuclide concentrations in the sediments would reflect average denudation rates of the upslope contributing area (Granger et al., 1996; Bierman and Steig, 1996). That ridge crest and basin averaged rates are similar suggests that the biogenic processes driving hillslope erosion are keeping up with the increased fluvial incision at the escarpment base, such that there is the suggestion for local steady-state where these rates are nearly equal.

Recent studies using low-temperature thermochronology and cosmogenic nuclides inferred denudational histories for passive margin escarpments, including a transect across the same field area that we are using here, and concluded that rift escarpments experience most of their erosion and retreat soon after rift development (Cockburn et al., 2000; Matmon et al., 2002; Persano et al., 2002). These studies provide important new constraints for the denudational histories of escarpments, which are used in modeling efforts that had previously predicted the same finding (Gilchrist et al., 1994; van der Beek and Braun, 1998). The mechanism suggested by Cockburn et al. (2000) and predicted by the above modeling studies, is that a major inland drainage divide fed rivers that rapidly eroded the newly formed escarpment shortly after formation. Studies from the southeastern Australia escarpment further north of our study area focused on the mechanisms of escarpment propagation, but could not resolve the greater than two orders of magnitude difference between inferred retreat rates of ~3 km/m.y. and denudation rates of 0.04–12 m/m.y. estimated since the time of rifting (Seidl et al., 1996; Weissel and Seidl, 1997, 1998). Rates of surface processes reported here and in Heimsath et al. (2000) are more than an order of magnitude lower than the inferred local escarpment retreat rate of ~500 m/m.y. (dividing the roughly 50 km distance between the coast and scarp lip by 100 m.y., the rough time since rifting), highlighting the need to resolve the discrepancy between inferred and observed rates of escarpment retreat. If, instead of using the gross estimate of horizontal retreat obtained by dividing distance from the coast by time since rifting, we use the geometric relationship between lowering rates and retreat rates (where retreat rate equals lowering rate divided by the tangent of the mean escarpment angle), then a contemporary retreat can be estimated. Specifically, lowering rates range from ~12 to ~36 m/m.y. (excluding tors) across the scarp with an average gradient of 0.25, suggesting an average retreat rate between ~40 and 140 m/m.y., which is an order of magnitude slower than the rate required to retreat the escarpment from the coastline at a continuous pace since rifting. If escarpments such as the one studied here did indeed retreat rapidly soon after rifting and then settle into a period of relative erosional stability,

as our measurements and the above thermochronology studies suggest, then a geomorphic mechanism needs to be discovered that can accomplish the initial rapid retreat.

CONCLUSIONS

Our study used 44 new measurements of the in situ–produced cosmogenic nuclide, ^{10}Be, combined with two previously published studies using 46 measurements of both ^{10}Be and ^{26}Al, all measured from bedrock, saprolite, and stream sediments, to enable a comprehensive quantification of the erosion rates and processes across the passive margin escarpment of southeastern Australia. These rates further our understanding of the surface processes shaping landscapes with different climatic and tectonic histories. Specifically, we have documented two new relationships between soil production and the overlying soil thickness, termed the soil production function. These two new functions, from the coastal lowlands and from the highlands near the study areas used for previous studies, agree remarkably well with the earlier findings. We then connect the lowlands with the highlands by reporting erosion rates from samples taken from two different transects across the escarpment face. The first transect samples the convex-up ridge crest leading upslope from the study area at the escarpment base to the highlands above the escarpment lip. The second transect begins near the headwaters of the major escarpment-dissecting river and samples small catchments draining the spur ridges from the highlands to just upslope of the scarp base study area. Rates from these transects define a linear decrease in erosion rate with elevation across the face of the escarpment, with an apparent peak in denudation rate at the scarp base, and agree with the rates determined by our soil production studies. We conclude that biogenic processes of soil production and removal are keeping up with other observed processes of debris flows and bedrock landsliding (that we did not quantify here) across the escarpment to set the overall rate of escarpment retreat. This rate is at least an order of magnitude less than previously inferred, long-term scarp retreat rates long suggested by workers focusing on the problem and therefore calls for the need to resolve the discrepancy between observed rates of landscape denudation and inferred rates of scarp retreat.

ACKNOWLEDGMENTS

We thank Rishi Satyadharma (Steve Bateman) and his family for continued access to and unbounded hospitality at the Nunnock River field area. Bill Dietrich, Ian Prosser, and Kuni Nishiizumi helped initiate this work across the escarpment, and continued discussions have helped our thinking immensely. Paul Rustomji sampled and helped to process the nuclide samples from the coastal lowland site, and we thank him. Comments by Mike Summerfield and an anonymous reviewer helped improve the original manuscript. Cosmogenic nuclide measurements and field support were funded by Dartmouth College and National Science Foundation grants DEB-0128995 and EAR-0239655 to Heimsath. Thirteen nuclide measurements for this study and all the previous analyses were partially performed under the auspices of the U.S. Department of Energy by Lawrence Livermore National Laboratory (LLNL) under contract W-7405-Eng-48, while the research schools of Earth Sciences and Physical Sciences and Engineering at the Australian National University supported the rest.

REFERENCES CITED

Ahnert, F., 1987, Approaches to dynamic equilibrium in theoretical simulations of slope development: Earth Surface Processes and Landforms, v. 12, p. 3–15.

Banfield, J.F., and Eggleton, R.A., 1989, Apatite replacement and rare-earth mobilization, fractionation, and fixation during weathering: Clays and Clay Minerals, v. 37, no. 2, p. 113–127.

Bierman, P.R., 1994, Using in situ produced cosmogenic isotopes to estimate rates of landscape evolution; a review from the geomorphic perspective: Journal of Geophysical Research, ser. B, Solid Earth and Planets, v. 99, no. B7, p. 13,885–13,896, doi: 10.1029/94JB00459.

Bierman, P., and Caffee, M., 2001, Slow rates of rock surface erosion and sediment production across the Namib Desert and escarpment, southern Africa: American Journal of Science, v. 301, no. April/May, p. 326–358.

Bierman, P., and Steig, E.J., 1996, Estimating rates of denudation using cosmogenic isotope abundances in sediment: Earth Surface Processes and Landforms, v. 21, p. 125–139, doi: 10.1002/(SICI)1096-9837(199602)21:23.0.CO;2-8.

Bishop, P., 1985, Southeast Australian late Mesozoic and Cenozoic denudation rates: A test for late Tertiary increases in continental denudation: Geology, v. 13, p. 479–482, doi: 10.1130/0091-7613(1985)13<479:SALMAC>2.0.CO;2.

Bishop, P., 1986, Horizontal stability of the Australian continental drainage divide in south central New South Wales during the Cainozoic: Australian Journal of Earth Sciences, v. 33, p. 295–307.

Bishop, P., 1988, The eastern highlands of Australia: The evolution of an intraplate highland belt: Progress in Physical Geography, v. 12, p. 159–182.

Bishop, P., and Brown, R., 1992, Denudational isostatic rebound of intraplate highlands: The Lachlan River valley, Australia: Earth Surface Processes and Landforms, v. 17, no. 4, p. 345–360.

Bishop, P., and Goldrick, G., 2000, Geomorphological evolution of the East Australian continental margin, *in* Summerfield, M.A., ed., Geomorphology and global tectonics: Chichester, Wiley, p. 227–255.

Bishop, P., Young, R.W., and McDougall, I., 1985, Stream profile change and long-term landscape evolution; early Miocene and modern rivers of the East Australian highland crest, central New South Wales, Australia: Journal of Geology, v. 93, no. 4, p. 455–474.

Brown, E.T., Stallard, R.F., Larsen, M.C., Raisbeck, G.M., and Yiou, F., 1995, Denudation rates determined from the accumulation of in situ–produced ^{10}Be in the Luquillo Experimental Forest, Puerto Rico: Earth and Planetary Science Letters, v. 129, p. 193–202, doi: 10.1016/0012-821X(94)00249-X.

Brown, R.W., Summerfield, M.A., and Gleadow, A.J.W., 2002, Denudational history along a transect across the Drakensberg Escarpment of southern Africa derived from apatite fission-track thermochronology: Journal of Geophysical Research, v. 107, no. B12, 2350, doi: 10.1029/2001JB000745.

Bryant, E.A., Young, R.W., Price, D.M., and Short, S.A., 1994, Late Pleistocene dune chronology; near-coastal New South Wales and eastern Australia: Quaternary Science Reviews, v. 13, no. 3, p. 209–223, doi: 10.1016/0277-3791(94)90026-4.

Burke, B.C., and Heimsath, A.M., 2003, Variations in saprolite chemical weathering signatures: Geological Society of America Abstracts with Programs, v. 35, no. 6, p. 258.

Carson, M.A., and Kirkby, M.J., 1972, Hillslope form and process: New York, Cambridge University Press, 475 p.

Chappell, J., 1991, Late Quaternary environmental changes in eastern and central Australia, and their climatic interpretation: Quaternary Science Reviews, v. 10, no. 5, p. 377–390, doi: 10.1016/0277-3791(91)90002-C.

Clark, D.H., Bierman, P.R., and Larsen, P., 1995, Improving in situ cosmogenic chronometers: Quaternary Research, v. 44, p. 367–377, doi: 10.1006/qres.1995.1081.

Cockburn, H.A.P., and Summerfield, M.A., 2004, Geomorphological applications of cosmogenic isotope analysis: Progress in Physical Geography, v. 28, p. 1–42, doi: 10.1191/0309133304pp395oa.

Cockburn, H.A.P., Brown, R.W., Summerfield, M.A., and Seidl, M.A., 2000, Quantifying passive margin denudation and landscape development using a combined fission-track thermochronology and cosmogenic isotope analysis approach: Earth and Planetary Science Letters, v. 179, no. 3–4, p. 429–435, doi: 10.1016/S0012-821X(00)00144-8.

Cox, N.J., 1980, On the relationship between bedrock lowering and regolith thickness: Earth Surface Processes and Landforms, v. 5, p. 271–274.

Culling, W.E.H., 1960, Analytical theory of erosion: Journal of Geology, v. 68, p. 336–344.

Culling, W.E.H., 1965, Theory of erosion on soil-covered slopes: Journal of Geology, v. 73, p. 230–254.

Davis, J.C., Proctor, I.D., Southon, J.R., Caffee, M.W., Heikkinen, D.W., Roberts, M.L., Moore, T.L., Turteltaub, K.W., Nelson, D.E., Loyd, D.H., and Vogel, J.S., 1990, LLNL/UC AMS facility and research program: Nuclear Instruments Methods in Physics Research, Section B, no. B52, p. 269–272.

Dietrich, W.E., Reiss, R., Hsu, M.-L., and Montgomery, D.R., 1995, A process-based model for colluvial soil depth and shallow landsliding using digital elevation data: Hydrological Processes, v. 9, p. 383–400.

Dietrich, W.E., Bellugi, D., Heimsath, A.M., Roering, J.J., Sklar, L., and Stock, J.D., 2003, Geomorphic transport laws for predicting landscape form and dynamics, *in* Wilcock, P., and Iverson, R., eds., Prediction in geomorphology: Washington, D.C., American Geophysical Union, p. 103–132.

Dodson, J., 1977, Late Quaternary palaeoecology of Wyrie Swamp, south-eastern South Australia: Quaternary Research (Washington, University, Quaternary Research Center), v. 8, no. 1, Richard Foster Flint memorial volume, p. 97–114.

Dodson, J.R., 1987, Mire development and environmental change, Barrington Tops, New South Wales, Australia: Quaternary Research, v. 27, no. 1, p. 73–81, doi: 10.1016/0033-5894(87)90050-0.

Dodson, J.R., and Wright, R.V.S., 1989, Humid to arid to subhumid vegetation shift on Pilliga Sandstone, Ulungra Springs, New South Wales: Quaternary Research, v. 32, no. 2, p. 182–192.

Dumitru, T.A., Hill, K.C., Coyle, D.A., Duddy, I.R., Foster, D.A., Gleadow, A.J.W., Green, P.F., Kohn, B.P., Laslett, G.M., and O'Sullivan, A.J., 1991, Fission track thermochronology; application to continental rifting of south-eastern Australia, *in* 1991 APEA conference; New concepts for old areas: Victoria, Australia, APEA Melbourne, p. 131–142.

Dumitru, T.A., Miller, E.L., O'Sullivan, P.B., Amato, J.M., Hannula, K.A., Calvert, A.T., and Gans, P.B., 1995, Cretaceous to Recent extension in the Bering Strait region, Alaska: Tectonics, v. 14, no. 3, p. 549–563, doi: 10.1029/95TC00206.

Dunai, T.J., 2000, Scaling factors for production rates of in situ produced cosmogenic nuclides: A critical reevaluation: Earth and Planetary Science Letters, v. 176, p. 157–169, doi: 10.1016/S0012-821X(99)00310-6.

Dunne, J., Elmore, D., and Muzikar, P., 1999, Scaling factors for the rates of production of cosmogenic nuclides for geometric shielding and attenuation at depth on sloped surfaces: Geomorphology, v. 27, no. 1–2, p. 3–11, doi: 10.1016/S0169-555X(98)00086-5.

Foster, D.A., and Gleadow, A.J., 1991, The architecture of Gondwana rifting in southeastern Australia; evidence from apatite fission track thermochronology, *in* Unrug, R., Banks, M.R., and Veevers, J.J., eds., Gondwana eight; Assembly, evolution and dispersal: (Conference Proceedings)Hobart, Tasmania, Australia, p. 597–603.

Gabet, E.J., 2000, Gopher bioturbation: Field evidence for nonlinear hillslope diffusion: Earth Surface Processes and Landforms, v. 25, p. 1419–1428, doi: 10.1002/1096-9837(200012)25:133.0.CO;2-1.

Gilbert, G.K., 1877, Report on the geology of the Henry Mountains (Utah): Washington, D.C., U.S. Government Printing Office, U.S. Geological Geographical and Survey of the Rocky Mountains Region, 170 p.

Gilchrist, A.R., Kooi, H., and Beaumont, C., 1994, Post-Gondwana geomorphic evolution of southwestern Africa: Implications for the controls on landscape developments from observations and numerical experiments: Journal of Geophysical Research, Solid Earth and Planets, v. 99, no. B6, p. 12,211–12,228, doi: 10.1029/94JB00046.

Gleadow, A.J.W., Kohn, B.P., Brown, R.W., O'Sullivan, P.B., and Raza, A., 2002, Fission track thermotectonic imaging of the Australian continent: Tectonophysics, v. 349, p. 5–21, doi: 10.1016/S0040-1951(02)00043-4.

Gosse, J.C., and Phillips, F.M., 2001, Terrestrial in situ cosmogenic nuclides: Theory and application: Quaternary Science Reviews, v. 20, p. 1475–1560, doi: 10.1016/S0277-3791(00)00171-2.

Granger, D.E., and Smith, A.L., 2000, Dating buried sediments using radioactive decay and muogenic production of ^{26}Al and ^{10}Be: Nuclear Instruments & Methods in Physics Research: Section B, Beam Interactions with Materials and Atoms, v. 172, no. 1–4, p. 824–828.

Granger, D.E., Kirchner, J.W., and Finkel, R., 1996, Spatially averaged long-term erosion rates measured from in situ–produced cosmogenic nuclides in alluvial sediment: Journal of Geology, v. 104, no. 3, p. 249–257.

Granger, D.E., Riebe, C.S., Kirchner, J.W., and Finkel, R.C., 2001, Modulation of erosion on steep granitic slopes by boulder armoring, as revealed by cosmogenic ^{26}Al and ^{10}Be: Earth and Planetary Science Letters, v. 186, p. 269–281, doi: 10.1016/S0012-821X(01)00236-9.

Harrison, S.P., 1993, Late Quaternary lake-level changes and climates of Australia: Quaternary Science Reviews, v. 12, no. 4, p. 211–231, doi: 10.1016/0277-3791(93)90078-Z.

Hayes, D.E., and Ringis, J., 1973, Seafloor spreading in the Tasman Sea: Nature, v. 243, p. 454–458.

Heimsath, A.M., Dietrich, W.E., Nishiizumi, K., and Finkel, R.C., 1997, The soil production function and landscape equilibrium: Nature, v. 388, p. 358–361, doi: 10.1038/41056.

Heimsath, A.M., Dietrich, W.E., Nishiizumi, K., and Finkel, R.C., 1999, Cosmogenic nuclides, topography, and the spatial variation of soil depth: Geomorphology, v. 27, no. 1–2, p. 151–172, doi: 10.1016/S0169-555X(98)00095-6.

Heimsath, A.M., Chappell, J., Dietrich, W.E., Nishiizumi, K., and Finkel, R.C., 2000, Soil production on a retreating escarpment in southeastern Australia: Geology, v. 28, no. 9, p. 787–790, doi: 10.1130/0091-7613(2000)028<787:SPOARE>2.3.CO;2.

Heimsath, A.M., Chappell, J., Dietrich, W.E., Nishiizumi, K., and Finkel, R.C., 2001, Late Quaternary erosion in southeastern Australia: A field example using cosmogenic nuclides: Quaternary International, v. 83–5, p. 169–185, doi: 10.1016/S1040-6182(01)00038-6.

Kershaw, A.P., D'Costa, D.M., McEwen Mason, J.R.C., and Wagstaff, B.E., 1991, Palynological evidence for Quaternary vegetation and environments of mainland southeastern Australia: Quaternary Science Reviews, v. 10, p. 391–401, doi: 10.1016/0277-3791(91)90003-D.

King, L.C., 1962, The morphology of the Earth: White Plains, New York, Oliver and Boyd, 726 p.

Kohl, C.P., and Nishiizumi, K., 1992, Chemical isolation of quartz for measurement of in-situ–produced cosmogenic nuclides: Geochimica et Cosmochimica Acta, v. 56, p. 3583–3587, doi: 10.1016/0016-7037(92)90401-4.

Lal, D., 1988, In situ–produced cosmogenic isotopes in terrestrial rocks: Annual Review of Earth and Planetary Sciences v. 16, p. 355–388.

Lal, D., 1991, Cosmic ray labeling of erosion surfaces: In situ nuclide production rates and erosion models: Earth and Planetary Science Letters, v. 104, p. 424–439, doi: 10.1016/0012-821X(91)90220-C.

Lal, D., and Arnold, J.R., 1985, Tracing quartz through the environment: Proceedings of Indian Academic Science (Earth and Planetary Sciences), v. 94, no. 1, p. 1–5.

Lal, D., and Peters, B., 1967, Cosmic ray produced radioactivity on the Earth: New York, Springer-Verlag, Encyclopedia of Physics, v. XLVI/2, p. 551–612.

Lambeck, K., and Stephenson, R., 1985, Post-orogenic evolution of a mountain range; south-eastern Australian highlands: Geophysical Research Letters, v. 12, no. 12, p. 801–804.

Lewis, P.C., and Glen, R.A., 1995, Bega-Mallacoota geological sheet, SJ/55-4, SJ/55-8, second edition: Sydney, Australia, Geological Survey of New South Wales, scale 1:250,000.

Linton, D.L., 1955, The problem of tors: The Geographical Journal, v. 121, p. 470–487.

Masarik, J., Kollar, D., and Vanya, S., 2000, Numerical simulation of in situ production of cosmogenic nuclides: Effects of irradiation geometry: Nuclear Instruments and Methods in Physics Research Section B-BEAM Interactions with Materials and Atoms, v. 172, p. 786–789.

Matmon, A., Bierman, P., and Enzel, Y., 2002, Pattern and tempo of great escarpment erosion: Geology, v. 30, no. 12, p. 1135–1138, doi: 10.1130/0091-7613(2002)030<1135:PATOGE>2.0.CO;2.

McAlpine, J.R., and Yapp, G.A., 1969, Climate of the Queanbeyan-Shoalhaven area; lands of the Queanbeyan-Shoalhaven area, ACT and NSW: Canberra, Australia, Land Resources Service, Commonwealth Science and Industrial Research Organization, p. 57–75.

Moore, M.E., Gleadow, A.J.W., and Lovering, J.F., 1986, Thermal evolution of rifted continental margins; new evidence from fission tracks in basement apatites from southeastern Australia: Earth and Planetary Science Letters, v. 78, no. 2–3, p. 255–270, doi: 10.1016/0012-821X(86)90066-X.

Nishiizumi, K., Winterer, E.L., et al., 1989, Cosmic ray production rates of ^{10}Be and ^{26}Al in quartz from glacially polished rocks: Journal of Geophysical Research, v. 94, p. 17, 907–17, 915.

Nishiizumi, K., Winterer, E.L., Kohl, C.P., Klein, J., Middleton, R., Lal, D., and Arnold, J.R., 1989, Cosmic ray production rates of ^{10}Be and ^{26}Al in quartz from glacially polished rocks: Journal of Geophysical Research, v. 94, no. B12, p. 17,907–17,915.

Nishiizumi, K., Kohl, C.P., Arnold, J.R., Klein, J., Fink, D., and Middleton, R., 1991, Cosmic ray produced ^{10}Be and ^{26}Al in Antarctic rocks; exposure and erosion history: Earth and Planetary Science Letters, v. 104, no. 2–4, p. 440–454, doi: 10.1016/0012-821X(91)90221-3.

Nishiizumi, K., Kohl, C.P., Arnold, J.R., Dorn, R., Klein, J., Fink, D., Middleton, R., and Lal, D., 1993, Role of in situ cosmogenic nuclides ^{10}Be and ^{26}Al in the study of diverse geomorphic processes: Earth Surface Processes and Landforms, v. 18, p. 407–425.

Nishiizumi, K., Finkel, R.C., Klein, J., and Kohl, C.P., 1996, Cosmogenic production of ^{7}Be and ^{10}Be in water targets: Journal of Geophysical Research, v. 101, no. B10, p. 22,225–22,232, doi: 10.1029/96JB02270.

Nott, J.F., 1992, Long-term drainage evolution in the Shoalhaven catchment, Southeast Highlands, Australia: Earth Surface Processes and Landforms, v. 17, no. 4, p. 361–374.

Nott, J.F., Idnurm, M., and Young, R.W., 1991, Sedimentology, weathering, age and geomorphological significance of Tertiary sediments on the far south coast of New South Wales: Australian Journal of Earth Sciences, v. 38, no. 3, p. 357–373.

O'Sullivan, P.B., Kohn, B.P., Foster, D.A., and Gleadow, A.J.W., 1995, Fission track data from the Bathurst Batholith—Evidence for rapid mid-Cretaceous uplift and erosion within the eastern Highlands of Australia: Australian Journal of Earth Sciences, v. 42, no. 6, p. 597–607.

O'Sullivan, P.B., Foster, D.A., Kohn, B.P., and Gleadow, A.J.W., 1996, Multiple postorogenic denudation events—An example from the eastern Lachlan fold belt, Australia: Geology, v. 24, no. 6, p. 563–566, doi: 10.1130/0091-7613(1996)024<0563:MPDEAE>2.3.CO;2.

Ollier, C.D., 1978, Tectonics and geomorphology of the eastern Highlands, *in* Davies, J.L., and Williams, A.J., eds., Landform evolution in Australasia: Canberra, Australian National University, p. 5–47.

Ollier, C.D., 1982, The Great Escarpment of eastern Australia: Tectonic and geomorphic significance: Journal of the Geological Society of Australia, v. 29, p. 13–23.

Ollier, C.D., 1995, Tectonics and landscape evolution in southeast Australia: Geomorphology, v. 12, no. 1, p. 37–44, doi: 10.1016/0169-555X(94)00075-3.

Ollier, C.D., and Marker, M.E., 1985, The Great Escarpment of southern Africa: Zeitschrift für Geomorphologie, Supplementband, v. 54, p. 37–56.

Pain, C.F., 1985, Morphotectonics of the continental margins of Australia: Zeitschrift für Geomorphologie, Supplement Band, v. 54, p. 23–35.

Persano, C., Stuart, F.M., Bishop, P., and Barfod, D.N., 2002, Apatite (U-Th)/He age constraints on the development of the Great Escarpment on the southeastern Australian passive margin: Earth and Planetary Science Letters, v. 200, no. 1–2, p. 79–90, doi: 10.1016/S0012-821X(02)00614-3.

Richardson, S.J., 1976, Geology of the Michelago 1:100,000 sheet 8726: Canberra, Australia, Geological Survey of New South Wales, Department of Mineral Resources and Development, 253 p.

Riebe, C.S., Kirchner, J.W., and Finkel, R.C., 2001, Strong tectonic and weak climatic control on long-term chemical weathering rates: Geology, v. 29, p. 511–514, doi: 10.1130/0091-7613(2001)029<0511:STAWCC>2.0.CO;2.

Riebe, C.S., Kirchner, J.W., and Finkel, R.C., 2003, Long term rates of chemical weathering and physical erosion from cosmogenic nuclides and geochemical mass balance: Geochimica et Cosmochimica Acta, v. 67, p. 4411–4427, doi: 10.1016/S0016-7037(03)00382-X.

Riebe, C.S., Kirchner, J.W., and Finkel, R.C., 2004, Sharp decrease in long term chemical weathering rates along an altitudinal transect: Earth and Planetary Science Letters, v. 218, p. 421–434, doi: 10.1016/S0012-821X(03)00673-3.

Seidl, M.A., Weissel, J.K., and Pratson, L.F., 1996, The kinematics and pattern of escarpment retreat across the rifted continental margin of SE Australia: Basin Research, v. 8, no. 3, p. 301–316, doi: 10.1046/j.1365-2117.1996.00266.x.

Small, E.E., Anderson, R.S., and Hancock, G.S., 1999, Estimates of the rate of regolith production using ^{10}Be and ^{26}Al from an alpine hillslope: Geomorphology, v. 27, no. 1–2, p. 131–150, doi: 10.1016/S0169-555X(98)00094-4.

Stephenson, R., and Lambeck, K., 1985, Erosion-isostatic rebound models for uplift; an application to south-eastern Australia: The Geophysical Journal of the Royal Astronomical Society, v. 82, no. 1, p. 31–55.

Stone, J.O., 2000, Air pressure and cosmogenic isotope production: Journal of Geophysical Research, v. 105, p. 23,753–23,759, doi: 10.1029/2000JB900181.

Stone, J.O., Ballantyne, C.K., and Fifield, L.K., 1998a, Exposure dating and validation of periglacial weathering limits, northwest Scotland: Geology, v. 26, no. 7, p. 587–590, doi: 10.1130/0091-7613(1998)026<0587:EDAVOP>2.3.CO;2.

Stone, J.O., Evans, J.M., Fifield, L.K., Allan, G.L., and Cresswell, R.G., 1998b, Cosmogenic chlorine-36 production in calcite by muons: Geochimica et Cosmochimica Acta, v. 62, no. 3, p. 433–454, doi: 10.1016/S0016-7037(97)00369-4.

Summerfield, M.A., 1999, Geomorphology and global tectonics: Chichester, Wiley, 357 p.

Taunton, A.E., Welch, S.A., and Banfield, J.F., 2000a, Geomicrobiological controls on light rare earth element, Y and Ba distributions during granite weathering and soil formation: Journal of Alloys and Compounds, v. 303, p. 30–36, doi: 10.1016/S0925-8388(00)00597-1.

Taunton, A.E., Welch, S.A., and Banfield, J.F., 2000b, Microbial controls on phosphate and lanthanide distributions during granite weathering and soil formation: Chemical Geology, v. 169, no. 3–4, p. 371–382, doi: 10.1016/S0009-2541(00)00215-1.

Thomas, M.F., 1989a, The Role of etch processes in landform development. I: Etching concepts and their applications: Zeitschrift für Geomorphologie, v. 33, no. 2, p. 129–142.

Thomas, M.F., 1989b, The role of etch processes in landform development. II: Etching and the formation of relief: Zeitschrift für Geomorphologie, v. 33, no. 3, p. 257–274.

Thomas, M.F., 1995, Models for landform development on passive margins; some implications for relief development in glaciated areas: Geomorphology, v. 12, no. 1, p. 3–15, doi: 10.1016/0169-555X(94)00082-3.

Tucker, G.E., and Slingerland, R.L., 1994, Erosional dynamics, flexural isostasy, and long-lived escarpments: A numerical modeling study: Journal of Geophysical Research, ser. B, Solid Earth and Planets, v. 99, no. B6, p. 12,229–12,243, doi: 10.1029/94JB00320.

Tucker, G.E., and Slingerland, R., 1997, Drainage basin responses to climate change: Water Resources Research, v. 33, no. 8, p. 2031–2047, doi: 10.1029/97WR00409.

Twidale, C.R., 1971, Structural landforms; landforms associated with granitic rocks, faults, and folded strata: Cambridge, The Massachusetts Institute of Technology Press, 247 p.

Twidale, C.R., 1985, Granite landform evolution; factors and implications, *in* Hans Cloos Kolloquim: Bonn, Germany, Geologische Rundschau, p. 769–779.

Twidale, C.R., 1993, The research frontier and beyond; granitic terrains: Geomorphology, v. 7, p. 187–223.

Twidale, C.R., and Vidal Romani, J.R., 1994, On the multistage development of etch forms: Geomorphology, v. 11, p. 107–124, doi: 10.1016/0169-555X(94)90076-0.

van der Beek, P., and Braun, J., 1998, Numerical modelling of landscape evolution on geological time-scales: A parameter analysis and comparison with the south-eastern highlands of Australia: Basin Research, v. 10, p. 49–68, doi: 10.1046/j.1365-2117.1998.00056.x.

van der Beek, P., and Braun, J., 1999, Controls on post-mid-Cretaceous landscape evolution in the southeastern highlands of Australia: Insights from numerical surface process models: Journal of Geophysical Research, v. 104, no. B3, p. 4945–4966.

van der Beek, P., Summerfield, M.A., Braun, J., Brown, R.W., and Fleming, A., 2002, Modeling post-break-up landscape development and denudational history across the southeast African (Drakensberg Escarpment) margin: Journal of Geophysical Research, v. 107, no. B12, 2351, doi: 10.1029/2001JB000744.

Weissel, J.K., and Hayes, D.E., 1977, Evolution of the Tasman Sea reappraised: Earth and Planetary Science Letters, v. 36, no. 1, p. 77–84, doi: 10.1016/0012-821X(77)90189-3.

Weissel, J.K., and Seidl, M.A., 1997, Influence of rock strength properties on escarpment retreat across passive continental margins: Geology, v. 25, no. 7, p. 631–634, doi: 10.1130/0091-7613(1997)025<0631:IORSPO>2.3.CO;2.

Weissel, J.K., and Seidl, M.A., 1998, Inland propagation of erosional escarpments and river profile evolution across the southeast Australian passive continental margin, *in* Tinkler, K.J., and Wohl, E.E., eds., Rivers over rock: Fluvial processes in bedrock channels: Washington, D.C., American Geophysical Union Geophysical Monograph 107, p. 189–206.

Wellman, P., 1979, On the Cainozoic uplift of the southeastern Australian highland: Journal of the Geological Society of Australia, v. 26, p. 1–9.

Wellman, P., 1987, Eastern highlands of Australia; their uplift and erosion: Brown Mountain: Journal of Australian Geology and Geophysics, v. 10, p. 277–286.

Wellman, P., and McDougall, I., 1974, Potassium-argon ages on the Cainozoic volcanic rocks of New South Wales: Journal of the Geological Society of Australia, v. 21, no. 3, p. 247–272.

Williams, A.G., Ternan, L., and Kent, M., 1986, Some observations on the chemical weathering of the Dartmoor Granite: Earth Surface Processes and Landforms, v. 11, p. 557–574.

Young, R.W., 1977, Landscape development in the Shoalhaven River catchment of southeastern New South Wales: Zeitschrift für Geomorphologie, Supplement Band, v. 21, no. 3, p. 262–283.

Young, R.W., 1983, The tempo of geomorphological change; evidence from southeastern Australia: Journal of Geology, v. 91, no. 2, p. 221–230.

Young, R.W., and McDougall, I., 1982, Basalts and silcretes on the coast near Ulladulla, southern New South Wales: Journal of the Geological Society of Australia, v. 29, no. 4, p. 425–430.

Young, R.W., and McDougall, I., 1993, Long-term landscape evolution—Early Miocene and modern rivers in southern New South Wales, Australia: Journal of Geology, v. 101, no. 1, p. 35–49.

Manuscript Accepted by the Society 23 June 2005

Printed in the USA